Biogeosciences Discuss., 10, 15455–15517, 2013
www.biogeosciences-discuss.net/10/15455/2013/
doi:10.5194/bgd-10-15455-2013

Biogeosciences Discussions
Open Access

Oxygen minimum zone of the open Arabian Sea: variability of oxygen and nitrite from daily to decadal time scales

K. Banse[1], S. W. A. Naqvi[2], P. V. Narvekar[2], J. R. Postel[1], and D. A. Jayakumar[2,*]

[1]University of Washington, School of Oceanography, Box 357940, Seattle, Washington 98195-7940, USA
[2]National Institute of Oceanography, Council of Scientific & Industrial Research, Dona Paula, Goa 403 004, India
[*]now at: Princeton University, M45 Guyot Hall, Department of Geosciences, Princeton, New Jersey, 08544, USA

Received: 15 August 2013 – Accepted: 23 August 2013 – Published: 30 September 2013

Correspondence to: K. Banse (banse@uw.edu)

Published by Copernicus Publications on behalf of the European Geosciences Union.

Abstract

The oxygen minimum zone (OMZ) of the Arabian Sea is the thickest of the three oceanic OMZs, which is of global biogeochemical significance because of denitrification in the upper part leading to N_2 and N_2O production. The residence time of the OMZ water is believed to be less than a decade. The upper few hundred meters of this zone are nearly anoxic but non-sulfidic and still support animal (metazoan) pelagic life, possibly as a result of episodic injections of O_2 by physical processes. The very low O_2 values obtained with the new STOX sensor in the eastern tropical South Pacific probably also characterize the Arabian Sea OMZ, but there is no apparent reason as to why the temporal trends of the historic data should not hold.

We report on discrete measurements of dissolved O_2 and NO_2^-, besides temperature and salinity, made between 1959 and 2004 well below the tops of the sharp pycno- and oxyclines near 150, 200, 300, 400, and 500 m depth. We assemble nearly all O_2 determinations (originally, 849 values, 695 in the OMZ) by the visual endpoint detection of the iodometric Winkler procedure, which in our data base yields about 0.04 mL L^{-1} ($\sim$ 2 µM) O_2 above the endpoint from modern automated titration methods. We find 632 values acceptable (480 from 150 stations in the OMZ). The data are grouped in zonally-paired boxes of 1° lat. and 2° long. centered at 8°, 10°, 12°, 15°, 18°, 20°, and 21° N along 65° E and 67° E. The latitudes of 8–12° N, outside the OMZ, are only treated in passing. The principal results are as follows: (1) an O_2 climatology for the upper OMZ reveals a marked seasonality at 200 to 500 m depth with O_2 levels during the northeast monsoon and spring intermonsoon season elevated over those during the southwest monsoon season (median difference, 0.08 mL L^{-1} [3.5 µM]). The medians of the slopes of the seasonal regressions of O_2 on year for the NE and SW monsoon seasons are -0.0043 and -0.0019 mL L^{-1} a^{-1}, respectively (-0.19 and -0.08 µM a^{-1}; $n = 10$ and 12, differing at $p = 0.01$); (2) four decades of statistically significant decreases of O_2 between 15° and 20° N but a trend to a similar increase near 21° N are observed. The balance of the mechanisms that more or less annually maintain the O_2 levels are still

BGD
10, 15455–15517, 2013

uncertain. At least between 300 and 500 m the annual reconstitution of the decrease is inferred to be due to lateral, isopycnal re-supply of O_2, while at 200 (250?) m it is diapycnal, most likely by eddies. Similarly, recent models show large vertical advection of O_2 well below the pycno-*cum*-oxycline. The spatial (within drift stations) and temporal (daily) variability in hydrography and chemistry is large also below the principal pycnocline. The seasonal change of hydrography is considerable even at 500 m.

There is no trend in the redox environment for a quarter of a century at a GEOSECS station near 20° N. In the entire OMZ the slopes on year within seasons for the quite variable NO_2^- (taken as an indicator of active denitrification) do not show a clear pattern. Also, future O_2 or nutrient budgets for the OMZ should not be based on single cruises or sections obtained during one season only. Steady state cannot be assumed any longer for the intermediate layers of the central Arabian Sea.

1 Introduction

Our paper addresses variability and climatology of dissolved oxygen (O_2) and nitrite (NO_2^-) from discrete samples collected between 1959 and 2004 in the upper oxygen minimum zone (OMZ) of the central Arabian Sea. The entire OMZ occupies approximately the 150–1000 m depth range and is the thickest of the three major OMZs of the open ocean. Between 1/4 and 1/3 of the total marine denitrification is estimated to occur in the water column, of which up to 1/3–1/2 may take place within the OMZ of the Arabian Sea (Codispoti et al., 2001; Bange et al., 2005). Naqvi et al. (2005: Table 9) estimated the contribution to the global marine pelagic denitrification by the Arabian Sea to be between 8 and 21 %. The principal denitrifying zone is located in the upper 1/3 of the OMZ where O_2 concentrations as determined by the visual endpoint detection of the Winkler titration fall below 0.06 mL L^{-1} (about 2.7 µM; however, see below). The zone is readily identifiable by the secondary NO_2^- maximum, which mostly is due to NO_3^- reduction and separate from the primary NO_2^- maximum that is more commonly found near the bottom of the euphotic zone (cf. Supplement Fig. S.3.1; Lomas and Lipschultz, 2006). Besides the release of N_2 as the end product through denitrification and anammox pathways (Dalsgaard et al., 2003, 2005; Kuypers et al., 2003; Ward et al., 2009; Ward, 2013), the O_2 deficiency enhances the production of nitrous oxide (N_2O), another intermediate of the nitrogen redox chemistry (Naqvi and Noronha, 1991; Devol et al., 2006; Naqvi et al., 2006).

The OMZ is not restricted to a particular range of temperature, salinity, or density and is essentially maintained by the balance between the supply of O_2 through eddy mixing and horizontal advection, principally from the southwest, and local consumption. The mean residence time of water appears to be less than a decade (Naqvi, 1987; Somasundar and Naqvi, 1988; Olson et al., 1993; Howell et al., 1997). Lam et al. (2011), though, deduced a residence time of a few decades. Accepting a short residence time, temporal O_2 changes should be discernible in historical data from four decades as analyzed here. Because small O_2 shifts at the generally quite low concentrations in the OMZ may suddenly stop or start denitrification, the temporal variability of the intensity and geographical extent of this OMZ are of global biogeochemical significance.

After we had largely completed our analysis of the historical O_2 data, we learned of the introduction to the field of the STOX sensor (Switchable Trace amount OXygen, Revsbech et al., 2009). Its detection limit is almost two orders of magnitude lower than that of the automated Winkler titration and will necessitate a re-assessment of the intensity of the oceans' OMZs. Titration was hitherto used worldwide for O_2 studies, including for the calibration of the O_2 probes attached to CTDs. Thamdrup et al. (2012) in February 2007 employed the sensor along a section from 28° to 5° S off the continental slope in the eastern tropical Pacific. In the OMZ core between about 100 and 300–350 m depth, O_2 was consistently undetectable on 10 of 12 stations (detection limit 0.01 μmol kg^{-1} or less). The authors found depletion to < 0.09 μmol kg^{-1} O_2 (~ 0.002 mL L^{-1}) to be normal in the core. Further, NO_2^- in the secondary nitrite maximum occurred only at < 0.05 μmol kg^{-1} O_2 (~ 0.001 mL L^{-1}), which is lower by at least an order of magnitude than the best automated endpoint detection of the Winkler titration or the colorimetric measurements (Codispoti et al., 2001). Thamdrup et al. (2012)

BGD
10, 15455–15517, 2013

Title Page
Abstract | Introduction
Conclusions | References
Tables | Figures
◀| |▶
◀ ▶
Back | Close
Full Screen / Esc
Printer-friendly Version
Interactive Discussion

concluded that the core of the OMZ off Peru is broadly functionally anoxic, because the observed low O_2 cannot sustain aerobic metabolism for any lengthy period. Ulloa et al. (2012) applied the term AMZ (Anoxic Marine Zone) to the region. Since metazoans like copepods are obligatory aerobes, we consider AMZ to mean a water column without animal zooplankton on a 24 h basis and use the term accordingly.

Advection adds O_2 at least occasionally to OMZs and AMZs, as noted off Peru by Thamdrup et al. (2012) and illustrated by Ulloa et al. (2012) for June 2007 off northern Chile. Measured by a drifting float profiling every 3 days, a counter-clockwise rotating eddy had depressed the pycnocline and enhanced O_2 through the entire core of the OMZ to about 500 m depth, while an adjoining eddy had raised better oxygenated water from below the core to about 150 m depth.

Because of the many samples with high concentrations of NO_2^- the OMZ of the Arabian Sea is expected to broadly present low oxygen conditions similar to those in the eastern tropical South Pacific. However, we know of only one instance when O_2 was measured using STOX in the region (September/October 2007, in Jensen et al., 2011: Supplement Fig. S.2). At three stations over depth intervals of several hundred meters, dissolved O_2 was $\leq 0.09\,\mu mol\,kg^{-1}$ ($\sim 0.002\,mL\,L^{-1}$), which was the detection limit of the sensor on the cruise. NO_3^- has always been found to be present in fairly high concentrations within the OMZ during the last eight decades, though, ruling out sulfidic anoxia in the water column, and metazoan plankton are present throughout, albeit in diminished numbers within the upper OMZ (Sect. 3.2.5). Thus this OMZ clearly cannot be characterized as an AMZ.

The OMZ and the deep NO_2^- maximum it contains, which is indicative of denitrification, were first discovered in the Arabian Sea by Gilson (1937). Numerous NO_2^- measurements during many subsequent expeditions showing values $> 0.5\,\mu M$ and up to $\sim 5\,\mu M$, that commonly occur in our data as well, imply that at least during the last 75 yr, the lowest O_2 concentrations in this OMZ must have been at nanomolar levels (Thamdrup et al., 2012), in contrast to all historical O_2 data including those used herein (Table S.1.b). The appreciable nitrate deficit resulting from the partial denitrification and

BGD
10, 15455–15517, 2013

anammox, ranging at its vertical maximum between 2 and 15 µM NO_3^-, has been discussed since the mid-1970s (e.g., Sen Gupta et al., 1976; see also Sect. 3.2.6). More recent is the demonstration that the OMZ has existed during much of the Holocene (Sect. 3.2.7).

So, today, is the OMZ of the Arabian Sea, or at least its core, functionally anoxic as suggested by Thamdrup et al. (2012) for the core of the OMZ of the eastern tropical South Pacific? Also, what to think of the historic O_2 data collated in our set with a lower detection limit of about 0.04 mL L^{-1} O_2 (∼ 2 µM) above the endpoint of modern automated methods, which is about 0.01 mL L^{-1} O_2 (∼ 0.5 µM)?

The answer to the first question is no. Metazoan (animal) zooplankton reside in the OMZ even where the median O_2 content, as determined by the Winkler procedure, is lowest (Sect. 3.2.5). Further, we will show by the 40 yr climatology in our wide longitudinal swath (Fig. 1) that the upper 200 (250?) m are seasonally being stirred, presumably by eddies (Sect. 4.1.2). At the 300 to 500 m horizons O_2 is advected annually from the side and reconstitutes the O_2 consumed during the SWM period (Sect. 4.2.1). Moreover, NO_2^- is largely observed only in the upper part of the OMZ, between 150–200 and 300–400 m depth, although the lower boundary of the secondary nitrite maximum could sometimes be as deep as 600–700 m in the northeastern Arabian Sea (Naqvi, 1987; Morrison et al., 1999). Importantly, in our data sets between 200 and 500 m, 21 % of 707 samples of boxes D1-G2 (without 500 m in D1, D2, see Table 2) contained zero to ≤ 0.02 µM NO_2^- (for details, see Sect. 3.2.5).Thus they were not next-to-fully depleted of O_2, and so denitrification was inhibited. In contrast, this percentage was 82 % of 255 samples outside the OMZ in boxes A1-C2 and the deepest horizon in the D-boxes. We also observe that the about 4/5 of our 707 samples coming from the 200 to 500 m horizons, which have significant amounts of NO_2^-, are unevenly distributed in space, as is the > 1/5 that contains too much O_2 to allow denitrification. Thus there is sufficient O_2 present in the core of the OMZ, although scattered and low, which not only sustains microbial life but also maintains a few copepod and other animal species year round, albeit at reduced concentrations (Sect. 3.2.6).

BGD
10, 15455–15517, 2013

In answer to the second question, we do not know of a reason why the temporal trends of O_2 to be presented herein should not hold. Were it not so, the ocean- and basin-scale sections of low concentrations of dissolved O_2 currently in the literature would not closely reflect the basin-wide distribution of nutrients. Therefore, we proceed here with using our less accurate data.

Below, we describe first the methods and data selection for temperature, salinity, oxygen, and nitrite in subsamples drawn from the same water bottle. Then we review and update the setting of the OMZ to 500 m depth, including the small-scale spatial and temporal (days to weeks) variability in order to provide perspective on the observations. The core of the paper addresses seasonal and four-decadal changes of O_2 and NO_2^-. We conclude with a section on the implications of the results.

2 Materials and methods

2.1 Data sources

The principal sources for our discrete observations of O_2 and NO_2^- together with temperature and salinity were the Indian and US national oceanographic data centers (INODC and NODC, respectively). Collections on some additional cruises conducted by India's National Institute of Oceanography but not yet incorporated in the INODC and NODC bases were also utilized. All data had been taken near 150, 200, 300, 400, and 500 m, within boxes of 1° lat. by 2° long. The boxes are centered at 8°, 10°, 12°, 15°, 18°, 20°, and 21° N along 65° E and 67° E (from A1 to G1 and B2 to G2, respectively, in Fig. 1). While the text and the figures refer to rounded nominal depths, the great majority of our data were collected within 5 % and in some cases within 10 % of the nominal horizons. In addition, we include some O_2 observations at exact nominal depths and the very few values from data centers that were already interpolated to them. The measurements used are listed in Supplement Table S.1.b together with the temperature and salinity of the samples.

We identify the seasons following the US JGOFS mode (Morrison et al., 1998) but the starting dates were lagged by one-half to one month: northeast monsoon (NEM), December-March; spring intermonsoon (SI), April–May; southwest monsoon (SWM), June–September; and fall intermonsoon (FI), October–November. The lag is introduced because the biochemical response at depth depends also on the downward transmission of surface signals by sinking particles.

2.2 Temperature and salinity

All temperatures and salinities accompanying the O_2 and/or NO_2^- data were taken at face value except that five hydrographic series (including the O_2 and NO_2^- values) were eliminated as occurring in exceptionally deep eddies (two series) or as clearly due to pre-trips of the entire bottle strings. A very few salinity records were dropped as false by being obvious outliers in *T*-*S* diagrams. To fill in large temporal gaps, a few measurements without O_2 and/or NO_2^- observations were taken from the data centers. Data from 329 and 332 stations with 1376 temperature and 1380 salinity values, respectively, were utilized (Table S.1.b). As in the case of O_2 and NO_2^-, the total includes some means of replicate casts at routine or drift stations. Supplement Tables S.2 and S.3 present the medians of temperature and salinity for all boxes and depths.

2.3 Oxygen

Our O_2 data were generated by the iodometric Winkler titration technique with visual end-point detection. This procedure was in general use until it was partially replaced by automated titration, by which also the CTD-attached O_2 probes were calibrated. In turn, the introduction of the STOX sensor by Revsbech et al. (2009), which has a detection limit about two orders of magnitude lower than the automated Winkler analysis, has opened a new era.

For our boxes we strove to collect all observations based on manual Winkler titrations with visual endpoint detection, but had to remove quite a number because of obvious bias as detailed below. Measurements by other methods, i.e., those involving automated (e.g., colorimetric or photometric) endpoint detection of the iodometric titration, were not considered, unless noted, because of systematic differences in the analytical results discussed below. Excluded thus are cruises 118 and 159 of R/V *Gaveshani*, as well as the observations from cruises 99 and 104 of R/V *Sagar Kanya* and all those by R/V *T. G. Thompson* and other recent expeditions. To our knowledge, for avoiding interference by nitrite, sodium azide was not added on any expedition except those by R/V *T. G. Thompson* (Morrison et al., 1999).

Almost all of our O_2 data were recorded in $\mathrm{mL\,L^{-1}}$, which we did not convert to µM or $\mathrm{\mu mol\,kg^{-1}}$, except for means and medians, because reporting the exact multiplication would have added a decimal place implying a false precision, whereas rounding off might have introduced errors in means and medians of sets of often only five to ten values. Original observations expressed as $\mathrm{\mu mol\,kg^{-1}}$ were retained but also stated as converted v/v or molar units.

Most data since the mid-1970s were collected by India's National Institute of Oceanography employing 60 mL bottles, adding 0.5 mL each of the two Winkler reagents, and analyzing with the visual starch-based endpoint detection procedure. The small amount of O_2 carried by the reagents was not subtracted and sodium azide (NaN_3) was not added to take care of NO_2^- interference in the Winkler titration. The lower limit of detection is approximately $0.05\,\mathrm{mL\,L^{-1}}$ (~ 2 µM). The correction for blanks, if any, for the other (non-Indian) data based on visual endpoints and used by us is unknown.

During the last two to three decades O_2 was analyzed with automated endpoint detection in the Winkler analysis (JGOFS manual; Anon., 1994). By comparing such measurements with visual endpoint detection in the same boxes during the same periods, we find an overestimate by $0.04\,\mathrm{mL\,L^{-1}}$ O_2 (~ 2 µM) (Supplement, Sect. 2). Without further evidence we generalize the difference as applicable to our entire material in Table S.1.b. In view of the low O_2 concentrations in the OMZ (Sect. 3.1.2), the bias is far from negligible.

BGD
10, 15455–15517, 2013

The accuracy in historical O_2 data may vary for a number of reasons. For quality control we used the accompanying NO_2^- values, all accepted at face value, and eliminated O_2 values > 0.10 mL L^{-1} when they were accompanied by NO_2^- values > 0.2 µM. As stated above, high NO_2^- is an indicator of denitrification, and if associated with substantial O_2 it implies overestimation of the latter (see Sect. 1; also Supplement, Sect. 2). The 0.2 µM contour was used by Naqvi (1991) to demarcate the boundaries of the suboxic zone in the Arabian Sea. We corrected apparent O_2 measurements < 0.10 mL L^{-1} accompanied by $NO_2^- \geq 0.2$ µM for nitrite interference (Wong 2012) and signified these by italics in Table S.1.b. Our cutoff of 0.2 µM NO_2^- for eliminating $O_2 > 0.10$ mL L^{-1} was rather subjective but seemed justifiable given the variability in NO_2^- blanks that may introduce errors up to ~ 0.05 µM. Of course, in view of the recently recognized much lower O_2 threshold for the onset of denitrification (Sect. 1) the cutoff is indeed arbitrary and only serves to sort our data collation. The 1 µM NO_2^- contour in our Fig. 1 is close to the 0.2 µM contour in Naqvi (1991).

From all boxes between about 150 and 500 m, 849 O_2 values based on visual endpoint detection from 205 stations were found (duplicate casts on the same station are averaged and not counted as such; also not included are rejected data from three cruises mentioned below). In the OMZ (boxes D1-G2), 695 observations or means were recorded. Of these, 215 values with $O_2 > 0.10$ mL L^{-1} accompanied by $NO_2^- \geq 0.2$ µM were rejected. The remaining 480 data points came from 150 stations. Included are 31 stations with 56 samples with $O_2 > 0.10$ mL L^{-1} not accompanied by NO_2^- analyses because there was no reason to reject them (of these, 14 came from ~ 150 m where higher O_2 values can be expected because of the proximity to the oxycline). The inclusion of the 56 points did not alter our conclusions except possibly the decadal slope at 400 m in F1 in 1963.

Rejected and not included in any of the enumerations were O_2 records from two cruises that were in their entirety far too high within the OMZ north of 14° to 15° N during the four decades under consideration (R/V *Priliv,* May 1967; R/V *Akademik Kurchatov*, May 1976), as well as those from the 22nd cruise of R/V *Akademik Vernadsky* of 1980.

BGD

10, 15455–15517, 2013

Oxygen minimum zone of the open Arabian Sea

K. Banse et al.

Here, all O_2 values $> 0.10\,mL\,L^{-1}$ from the OMZ were accompanied by $NO_2^- > 0.2\,\mu M$, suggesting similar overestimates for the remaining determinations. Also dropped at the outset were several single O_2 values from other expeditions that appeared unreasonably high from the context, e.g., as compared to values from adjoining depths, or which came from transition layers with strong gradients.

The totals are 632 accepted measurements from 196 stations between 8° and 21° N (Table S.1.b). Table 1 presents the numbers and medians of these O_2 values for all boxes and depths.

2.4 Nitrite

Because the O_2 values within the OMZ are often very close to the lower limit of detection and hence perhaps not as precise as is desirable, we use NO_2^- as a surrogate of near-absence of O_2. On all cruises nitrite was determined following Bendschneider and Robinson (1952) or variants thereof. In contrast to the O_2 observations, the data from the U.S. JGOFS and WOCE programs were also included in our study. For the five horizons under consideration, 1191 data points from 292 stations (949 from 227 stations in the OMZ) were utilized, all analyses having been taken at face value (Table S.1.b). These totals comprise some averages of two or three replicate casts per station, as well as means of ≥ 4 (up to 28) replicated casts within the same day or consecutive days at fixed positions. Most of the high NO_2^- values were $< 5\,\mu M$ except a few that exceeded this concentration (maximum 6.2 µM). One outlier of 10.2 µM is found at 200 m in Box E2 in July 1970. Table 2 presents the numbers of samples and the medians for all boxes and depths.

2.5 Statistics

Seasonal and decadal changes were investigated by linear regression analysis with the independent variable (dates, i.e., year and month) known, and parametric statistics without testing for normality and homoscedasticity. Significance of differences between medians or groups of data was assessed by the non-parametric rank test (Wilcoxon T test = Mann-Whitney U test). Because the latter mostly addressed clear differences between two data sets, one-tailed tests were usually applied. In neither approach did those values that were based on means, weight the statistics. Our statements about significance of "differences between medians" are shorthand for "tests for significance of differences between two sets of independent values." The p values reflect the distribution of the variables tested, but also the often low number of samples. Because so many sets are small, reporting even $p = 0.2$ seems appropriate, but is not intended to serve as proof!

3 Results and discussion

3.1 Broad setting

The area of study lies, strictly speaking, between 7.5° and 21.5° N and 64° to 68° E (Fig. 1), but the southern boxes (A–C, 8–12° N), which are outside the suboxic OMZ, are treated only in passing. Sketching the general setting of the Arabian Sea, we note that previously the two monsoons were thought to force reversal of surface currents seasonally over the entire basin. Actually, much of the western half of the Arabian Sea is full of cyclonic and anticyclonic, quasi-geostrophic mesoscale eddies and fronts with their associated meandering currents (Flagg and Kim, 1998; Shankar et al., 2002; Artamonov, 2006; Resplandy et al., 2011). The new insight is illustrated by maps of sea level anomalies (SLAs, Kim et al., 2001), sea surface height (Fischer et al., 2002; Weller et al., 2002; Resplandy et al., 2011), and geopotential anomalies (Artamonov, 2006). The eddies and fronts may reach 500 m depth (e.g., Artamonov, 2006: Figs. 3.15C–F, 3.16B; Bobko and Rodionova, 2006: O_2 at 300 m in Fig. 5.6, NO_3^- section in Fig. 5.8B). In addition, the salinity and temperature (CTD) profiles at stations in the northern boxes down to σ_t near 26 kg m^{-3} (roughly 200 m depth) show many salinity spikes in the pycnocline (see Figs. 2 and 8) from interweaving of relatively thin layers of varying salinity, presumably with varying biochemical histories. The cause probably is dense water from winter convection subducted and advected horizontally, then preserved in the pycnocline (e.g., Banse and Postel, 2009). Between σ_t of about 26–27 kg m^{-3}, similar layering is due to the intrusion from the Persian Gulf (the Persian Gulf Water, PGW, see Supplement Sect. S.3). The overall result of, especially, the hydrographic processes is substantial variability even within stations replicated during one to three days (Sect. 3.2.4) and is superimposed over marked seasonality even below the permanent thermocline (Sect. 4.1.2). Resplandy et al. (2011) in an eddy-resolving (1/12°) model showed the large role of vertical nutrient supply by eddies. However, as noted, e.g., by Shankar et al. (2002), the regularity of the monsoons makes features like "monsoon currents", which dominated the previous views of the circulation of the upper Arabian Sea, still stand out, including their relation to the depth of the principal thermocline. For other background, Wiggert et al. (2005) reviewed biogeochemical pelagic processes. Ramaswamy and Gaye (2006, Sta. EAST near 15° N, 65° E) described ten years of biogenic vertical flux at almost 3000 m depth.

The study region is largely outside the strong physical and biogeochemical activity offshore of the Arabian Peninsula and near the Murray Ridge. Similarly on its eastern side, our meridional band is largely beyond the influences of the sea level changes, currents, and Kelvin waves near the Indian Subcontinent. However, during the SWM period coastal upwelling reigns in the "meso-eastern-boundary-current regime" along the west coast of India, without the large eddies and offshore-drawn filaments as off the western side of the basin. Associated with the upwelling is the north-setting undercurrent, which advects O_2 poleward. Naqvi et al. (2006) reported low salinity and elevated O_2 near the continental slope off Goa (15° N) even in December in 1998 after the SWM had lasted unusually long and the surface flow was still directed toward the equator. Resplandy et al. (2012) in their eddy-resolving model generate the undercurrent below about 150 m depth and stress the importance of poleward O_2 advection along the continental slope.

BGD
10, 15455–15517, 2013

The general distribution of salinity and O_2 along 64° E as depicted by Olson et al. (1993: Fig. 2) for 1986 is probably valid also for 65° E. Between 200 and 500 m depth the median temperatures at each depth horizon increase with monotonous slopes by 2–3 °C, with the medians along 67° E (boxes B2–G2; Table S.2) tending to be cooler by a few tenths of a degree than those along 65° E (boxes A1–G1). Little more will be said about temperature. Between about 7° and 10° N the salinity below the bottom of the pycnocline at individual stations varies little with depth to at least 800 m but increases northward from ca. 35.2 to 35.3–35.4. To the north of 10° or 12° N up to 21° N, and between 150 and 500 m depth, the median salinities at each horizon increase with monotonous slopes to 35.9–36.0 (35.8 at 500 m near 65° E; Table S.3). In the OMZ the median salinities tend to be slightly lower along 67° E than in the western (along 65° E) boxes.

Over the range of about 7° to 10° N, near and somewhat below 200 m, O_2 as measured prior to the advent of the STOX probe declines from about 2 to about 0.4 mL L^{-1} (~ 90 to 18 µM; cf. Wyrtki, 1971: tables 441 and 502; see also the numerous significant differences among median O_2 values between the C and D boxes at 10° and 12° N, respectively, in Table 1). Naqvi et al. (1993) noted that the transitional zone is observed between these two latitudes, which during 1995 was only one degree wide. The position seems to be fairly stable in time, probably owing to the distribution of wind stress and the resulting quasi-zonal circulation (Warren, 1994; but see the section for the SWM in de Sousa et al., 1996, and Supplement, Sect. S.1). The very steep horizontal O_2 gradients at the southern edge of the upper half of the OMZ in our meridional band, not described previously, are to be treated by Banse and Postel (in preparation).

3.2 Setting of the OMZ

3.2.1 General hydrography

We focus on the OMZ poleward of 12° N. Our 150 m, uppermost horizon is below the salinity maximum of the non-seasonal pycnocline near a σ_t of 24 kg m^{-3} and below

BGD
10, 15455–15517, 2013
Oxygen minimum zone of the open Arabian Sea
K. Banse et al.

the sharp oxycline, which is the upper border of the OMZ. The depths of these clines vary seasonally (Colborn, 1975; Molinari et al., 1986), being deep in the SWM and, in the north, also during the NEM. The climatological depths of the bottom end of the steep vertical gradients of temperature, salinity, and oxygen occur somewhat above the 200 m horizon (see Fig. 2 as an example). Much of the OMZ has only weak vertical gradients of O_2, but zooplankton species may be layered, perhaps responding to these gradients, as found for copepods by Böttger-Schnack (1997) and Wishner et al. (1998).

Resplandy et al. (2012) with their eddy-resolving model studied the factors that control the O_2 balance in the OMZ. For a depth range of 250–300 m their computed median O_2 utilization rate was 2.8 µmol L^{-1} a^{-1} (range, 2.1–6.8 [0.06 mL L^{-1} a^{-1} (0.05–0.15)], Resplandy, in litt., July 2013; cf. their Fig. 6a CAS). They also reported for the NEM and SWM that the amplitude of seasonal O_2 change from vertical eddy-driven advection was several times that from biological consumption. Similarly, McCreary et al. (2013) in a non-eddy resolving (0.5°) model determined the large role of lateral O_2 advection to the central Arabian Sea. Neither paper addressed shifts on the climatological scale as we do here.

3.2.2 Oxygen

The intense (suboxic) OMZ extends from north of the C-boxes (12° N) poleward, although in September 1994 the depths at and slightly above 200 m in our Box C1 were part of this zone (R/V *T. G. Thompson* cruise TN039; see also the variable latitude of the denitrification zone in Naqvi, 1991). In the OMZ, the median visual Winkler O_2 levels are often below 0.1 or even 0.05 mL L^{-1} (Table 1). The many significant differences in the table between the 150 and 200 m horizons suggest restricting our treatment of the OMZ to the 200 to 500 m levels but adding the 150 m level in the D-boxes (15° N). The medians for the four deeper horizons range only between 0.04 and 0.15 mL L^{-1} O_2. Within the upper OMZ as studied here, the vertical gradients tend to be small; more often than not the differences between depth horizons are insignificant, as are the

BGD
10, 15455–15517, 2013

north-south differences with the exception of the G-boxes (Table 1). Regarding zonal differences, the means of the annual medians of the depths in the four western boxes are all higher than those of the eastern boxes, but the ranking of the medians in Table 1 shows significant differences only at 200 and 400 m ($p = 0.01$ and 0.2, respectively).

3.2.3 Nitrite and dinitrogen

Within the OMZ and in contrast to O_2, Table 2 shows many significant depth differences for NO_2^- in spite of the great variability of concentrations. The values are high at and poleward of 15° N except near 150 m. At 15° N (D-boxes), however, the high NO_2^- values at the 150 m horizon indicate fairly intense denitrification in conjunction with low oxygen. In contrast, there is little denitrification at 400 and 500 m at 15° N and little in the E-boxes at 500 m depth, reflecting the trends to slightly higher O_2 (medians, 0.10–0.13 mL L^{-1}, Table 2). For the same reason, the NO_2^- medians at 300 and 400 m in Box G1 decline relative to the adjoining Box F1. The low medians at 150 m in boxes E1 and F2 and at 400 m in the D-boxes, though, hide the fact that several to many high values were present along with zero concentrations (see Table S.1.b). The map of high and low values of NO_2^- at the 250 m horizon in Bobko and Rodionova (2006) from the central and northern Arabian Sea illustrates the role of downwelling from eddies to appreciable depths (cf. Artamonov, 2006).

Denitrification to N_2 (dinitrogen) rather than the anammox route was found to be the dominant source of loss of fixed nitrogen in the Arabian Sea by Ward et al. (2009, with earlier references; Bulow et al., 2010). In contrast, Lam et al. (2011) stressed the anammox pathway in the nitrogen cycling leading to N_2 losses in OMZs. Note that while anammox is an autotrophic process, both NO_2^- and NH_4^+ are largely derived from the heterotrophic decomposition of organic matter and therefore dependent on the supply of the latter. Ward (2013) reviewed new laboratory work showing the importance of the C : N ratio of the substrate, so that we believe that the debate about which pathway toward N_2 dominates in the Arabian Sea may be close to solution.

BGD
10, 15455–15517, 2013

3.2.4 Day-to-day and weekly variability

The highly dynamic nature of the hydrography creates temporal as well as spatial variability even in the central Arabian Sea at the same stations with repeated casts and is especially noticeable on week-long drift stations. For the area treated herein, previous papers emphasized temperature (isopleths, twice for four days in Box E2 (Ramesh Babu et al., 1981), as well as one and two weeks of mean isopleths of four stations centered in Box C1, both to 200 m (Rao, 1987), or temperature and salinity for 13 days (Prasanna [S.P.] Kumar et al., 2001; Naqvi et al., 2002).

In Table 3 the first two examples present among-days variability for temperature, salinity, O_2, and NO_2^- on stations near Box D1 and in Box E1, each maintained within 1–2 km. The standard deviations (S.D.) for O_2 are absolutely small, but may be as high as the low means. On both stations the variability of NO_2^- at 200–400 m is very large (the variance being larger than the mean), in part because of zero values but in part so even among the high concentrations, as will also be apparent in later sections. Measurements with fewer repeats on seven other locations in our data sets, including US JGOFS cruises, other than the following ones show similar variability. The third set of data in Table 3 come from a drift station near 21° N, where temporal and spatial variability change cannot be separated, but the spatial range of almost half a degree is relevant to comparisons of stations on sections with one-degree spacing (see also Supplement Fig. S.3.1).

The fourth example (Fig. 2) illustrates within-station and –day variability of hydrography south of Box D2 by 16 casts during a 28 h drift of about 41 km extent where spatial and temporal inhomogeneity came into play. The *T*-*S* diagram for the first 8 h (Fig. 2c) shows massive replacement of water between about 100 and 300 m, below the principal pycnocline.

Last, an inkling of large-scale distributions is provided by the already referred map of NO_2^- at 250 m depth on a one-half to two-thirds degree grid during the spring inter-

Discussion Paper | Discussion Paper | Discussion Paper | Discussion Paper |

BGD

10, 15455–15517, 2013

monsoon of 1990, coupled with the associated O_2 at the horizon and vertical sections indicating deep-reaching eddies in Bobko and Rodionova (2006: Figs. 5.6 and 5.11B).

In conclusion, a number of relatively small water masses with apparently different biochemical history are often present on the same density surfaces. This geographical heterogeneity is also to be expected in regional surveys or in interannual studies at fixed locations. Therefore, data from a few stations must not be over-interpreted.

3.2.5 Oxygen and nitrite co-occur temporally

The observations about hydrographic variability support our assumption set forth in Sect. 1 that O_2 and NO_2^- may co-exist temporally in the OMZ. Of course, they exclude each other spatially below the O_2 threshold for the onset of denitrification of $< 0.002\,\mathrm{mL\,L^{-1}}$ ($< 0.09\,\mu$M). As stated, 20 % of 646 samples contained $\leq 0.02\,\mu$M NO_2^-; the majority showed zero or 0.01 µM NO_2^-; the averages include NO_2^- not accompanied by O_2 data (Table S.1.b). In view of the aforementioned salinity spikes reflecting stratification (also Fig. 2), we visualize the dimensions of such patches horizontally to be much larger than vertically. On the average the patches must last many months, if not a year, such that planktonic animals (e.g., copepods) live and persist in an otherwise nearly anoxic milieu of a few tens of nanomoles of O_2 (see also the large "patches" free of NO_2^- at the end of Sect. 3.2.4). The average turnover time of NO_2^- in the central Arabian Sea of 49 ± 20 years estimated by Lam et al. (2011) seems way too long by our lines of argument, even when the obvious question of spatial scale is neglected.

3.2.6 Animal life

Metazoan zooplankton, which by its nature requires dissolved O_2, is found year-round in this OMZ. As remarked above, $NO_2^- \leq 0.02\,\mu$M (i.e., zero within the precision of the analysis) was measured in one-fifth of our samples from the 200 to 400 m horizons of the upper OMZ with its nitrite maximum. Thus enough O_2 is present in such samples

BGD
10, 15455–15517, 2013

to prevent denitrification and is sufficient to maintain a reduced number of species and specimens.

The following is merely to demonstrate that the OMZ harbors resident metazoans (additional reports in Supplement, Sect. S.4). Only nighttime data are considered, which exclude the diel migrators among plankton and nekton entering the top of the OMZ during daytime but which during the night in the mixed layer pay off the O_2 debt incurred at depth. Wishner et al. (1998) reported on divided hauls in 50 or 25 m steps at 5–6 stations in the upper OMZ during four seasons of 1995. Wet weights (preserved) at four offshore stations showed a distinct minimum of the order of 1 mg m^{-3} between about 200 and 400 m depth without clear seasonality. A secondary biomass maximum with about a tenfold increase occurred down to about 750 m. Specimen numbers per 1000 m^3 of individual species of calanoid copepods (adults and identifiable copepodites, *op. cit.*: Fig. 9) were several tens up to 100 in the 300 to 450 m depth interval and several tens to several hundreds up to 1000 in the slightly better oxygenated 500 to 750 m interval ($O_2 \sim 0.05$–0.015 mL L^{-1}, $\sim$2.3–4.5 µM). Their work stresses the response of species to small vertical O_2 changes, which leads to marked vertical zonation. The largest number of species in the lower OMZ was observed at $O_2 > 0.14$ mL L^{-1}. (These O_2 values were obtained with automated Winkler titration and with azide added to suppress NO_2^- interference; they are about 0.04 mL L^{-1} lower than those used in the bulk of this paper.) Smith and Madhupratap (2005) reviewed the copepod species preferentially or exclusively found in the OMZ, after summarizing more observations about the biomass minimum in the upper OMZ (see also Supplement, Sect. S.4).

The animal distribution in the upper OMZ of the Arabian Sea is not unique. Similar features, including the minima of biomass and number of species, are found in the OMZ of the Costa Rica Dome of the eastern tropical Pacific, including the secondary maximum of biomass and species occurrence in the lower part of the OMZ (Saltzman and Wishner, 1997). In the same region, Vinogradov et al. (1991), using plankton hauls and visual observations from a submersible, confirmed the similarity of vertical patterns

BGD
10, 15455–15517, 2013
Oxygen minimum zone of the open Arabian Sea
K. Banse et al.

between the Arabian Sea and the Costa Rica Dome but added the large contribution of biomass by gelatinous animals, which are a part of the OMZ fauna. Jelly-like animals accounted for 92 % of wet mass and 16 % of carbon to the meso- and macroplankton in the upper 500 m, omitting very large (> 15 cm) but rare medusae and ctenophores (see also Hamner et al., 1975; Ignatyev, 2006, in Supplement, Sect. S.3).

In conclusion of this sub-section, even the upper OMZ of the Arabian Sea is biologically not functionally anoxic, in contrast to the suggestion by Thamdrup et al. (2012) for much of the upper OMZ in the eastern South Pacific.

3.2.7 Nitrate deficit

The maximum of the NO_3^- deficit resulting from denitrification is also observed in the core of the OMZ, although tending to be a few tens of meters deeper than that of NO_2^- (Morrison et al., 1999: Fig. 8; the deficit was calculated by the "NO" approach, which below about 250 m depth might yield slight overestimates, see Naqvi and Sen Gupta, 1985: Fig. 2; Mantoura et al., 1993; also Chang et al., 2012). The maximal values in a season or a cruise range between about 2 and 15 µM. As illustrated by Morrison et al. (1999) for 1995, the deficit declines toward depth and vanishes by 600–900 m, while NO_2^- is not observed below 350 m depth (below 600 m at one of their four stations). However, note that the presence of an NO_3^- deficit does not reflect ongoing anoxia. Rather, the deficit regularly observed in the OMZ well below the deficit maximum, not accompanied by NO_2^-, is apt to be due to mixing downward from the depth of maximum. In the northeastern Arabian Sea, Naqvi et al. (1990) observed lower NO_3^- deficits during the SWM period of 1987 than during the NEM period of 1988 (2–3 µM to 8–9 µM, respectively).

The denitrification in the OMZ always leaves > 10 µM (usually ≫ 15) NO_3^- behind, which excludes the presence of H_2S. So, at least since the NO_3^- estimates by the R/V *Mabahiss* of 1933–1934 (Gilson, 1937) sulfidic anoxia has not occurred in the water

BGD
10, 15455–15517, 2013

Oxygen minimum zone of the open Arabian Sea

K. Banse et al.

column of the open Arabian Sea. Soviet records from the late 1950s and early 1960s of free H2S were based on an inadequate analytical method

3.2.8 Age of OMZ

Where the OMZ touches the continental slope, the sediment turns truly anoxic, hence macrofauna and bioturbation are absent (cf. review by Cowie and Levin, 2009). Regular compositional changes of settling material, as in the monsoon climate due to seasonality of plankton blooms and atmosphere- and river-supplied particles, result in annual, dateable varves. At a site off Karachi at 695 m depth, von Rad et al. (1999) observed a 5000 yr record of varved sediment starting at the sediment surface, but bioturbation was found below the earliest varve. From a pair of such cores taken at 316 m depth close by, Staubwasser et al. (2002; location in von Rad et al., 1995) concluded that the OMZ anoxia of the Arabian Sea started near 7300 BCE, which is supported by Thamban et al. (2007) from a core taken from 500 m depth on the Indian margin at 17°45′ N. The water below the OMZ has been oxygenated for at least the last 185 000 yr (Schenau et al., 2002).

4 Seasonal and decadal variability in the OMZ

Besides a *T*-*S* diagram of seasonal medians for the boxes (Fig. 3), the principal method of study is linear regression of the variable of interest on year (decimal fractions according to the month of observation). Decadal changes of temperature are not considered because linear regressions of sampling depth on year unexpectedly showed positive or negative trends. We neglect this source of possible bias for salinity, oxygen, and nitrite because of the much smaller vertical gradients at the horizons of concern.

BGD
10, 15455–15517, 2013

4.1 Temperature and salinity

4.1.1 Temperature

By the climatology of temperature of the upper 500 m, the 20 °C isotherm in the middle of the thermocline in our region moves seasonally by about 50 m (Molinari et al., 1986). Ramesh and Krishnan (2005) studied the seasonal downward transport of heat to ≥ 200 m as zonal averages between 50 and 70° E, for 0–20° N. They calculated that downwelling from convergence and horizontal advection, and the deepening and cooling of the upper layer coupled with strong vertical diffusivity from wind-caused turbulence, warmed the thermocline near 150, 200, and 250 m depths south of 12–13° N by about 1.2, 0.9, and 0.4 °C, respectively. Their Figs. 6, 8, and 9 also illustrate that the OMZ area of our study is largely outside the centers of the greatest hydrographic and associated changes in the western and southern Arabian Sea. Finally, the 2 yr time series by an Argo float launched at 12° N, 65° E and slowly drifting toward the southeast (Prakash et al., 2012) illustrates an apparently seasonal vertical shift of the top of the oxycline, the extremes ranging between 35–40 and 130 m depth (during the early winter monsoon and the spring intermonsoon, respectively).

4.1.2 Temperature-salinity relations

Our *T*-*S* diagram (Fig. 3) is based on medians of discrete data and presents the climatology for the OMZ in our meridional swath. The patterns of the two upper depths down to the isopycnals (σ_t) of 26.3–26.4 kg m^{-3} differ strikingly from those of the 300 to 500 m horizons. The former are dominated by seasonal, seemingly diapycnal warming to > 200 m depth (but < 300 m) in boxes B–G, extending well below the permanent pycnocline. In contrast, the three lower horizons exhibit clear isopycnal, seasonally periodic change at and poleward of the D-boxes, i.e., in the OMZ. Box C1 (12° N) at least at the 300 m horizon seems to follow this “deep” pattern. In the B-boxes (10° N) the seemingly diapycnal warming is observed even at 500 m, where the median temperatures ranges seasonally by 0.4–0.5 °C; the maximal and minimal values differ significantly in Box B2.

As expected from the climatology of Ramesh and Krishnan (2005: Fig. 4) for 150 and 200 m, the lowest median temperatures at these horizons tend to occur during the NEM, while the highest medians are found during the SI or SWM at 150 m up to 20° N (Boxes F1, F2) and at 200 m to 18° N (Box E1; at 200 m also in G1, 21° N, but not at 150 m). At the 300 m horizon in Box C1 and the D-boxes the weak temperature rise of the SWM is accompanied by a marked increase of salinity. Regrettably, no or insufficient (< 4 pairs) observations are available in all these boxes for the FI season for seeing whether the points return to the vicinity of the NEM (winter) values, as they do (or tend to do) in Box G1 at all depths.

According to the eddy-resolving model of Resplandy et al. (2011), the diapycnal heat transport demonstrated in Fig. 3 between 12 and 21° N is principally due to vertical advection and mixing by eddies but less so to horizontal advection. The apparently efficient mechanism(s) transmitting heat and, presumably, O_2 to the 150 m and 200 m horizons during the SI is not obvious, when the seasonal heating forms a thermocline in the upper 50 m or so.

At the 300 to 500 m horizons temperature and salinity increase and decrease in a periodic, isopycnal manner (Fig. 3). Both properties tend to be highest during the SI and SWM periods, as is the case for temperature also at the upper horizons. Note the somewhat elevated salinities at 300 m, relative to the two deeper horizons at a density close to that of the Persian Gulf intrusion from Box C1 (12° N) poleward. At depth, most temperature differences between the warmest and coolest seasons in the E- to G-boxes are significant, in part highly so ($p = 0.01$ to 0.05). The increases suggest horizontal advection, with more northerly water tending to be present during the SI period. The salinity increases tend to be more pronounced in the western boxes.

For boxes D1, D2, and G1, zonal seasonal data means and medians of temperature and salinity were also drawn from the averages in the World Ocean Data Base 2001 (Levitus et al., 2002; http://iridl.ldeo.columbia.edu/SOURCES/.NOAA/.NODC/.WOA01/).

BGD
10, 15455–15517, 2013

They indicate mild east-west gradients, with both variables tending to increase toward the west, which for temperature is in contrast to Fig. 3. The temperature maxima occur during the SI or SWM seasons. Further, in Box D2 between 250 and 500 m the FI period exhibits large salinity increases (0.05–0.1) accompanied by slight declines of temperature. Similar temperature decreases are observed in Box D1. In view of the critique by Bianchi et al. (2012) regarding artifacts arising from averaging and interpolating of O_2 data as used in the World Ocean Data Base, which in part applies to other variables, we lean toward giving more credence to our own medians, which are simply based on discrete samples.

Disregarding the small differences between our and Levitus' data, the principal conclusion from Fig. 3 for the OMZ (Boxes D–G) is the evidence of significant seasonal, periodic advection along isopycnals at 300–500 m depth, most marked during the SI and/or the SWM periods. Because temperature and salinity together increase at that time, the transport direction must be from the northern to the southern quadrants.

4.1.3 Decadal change of salinity

The general distribution of salinity was described earlier. For the climatological change, Supplement Table S.4 provides the regression slopes for salinity on years for all boxes and depth ranges for 3–4 decades, while Table S.5 presents seasonal regression on years for the OMZ when ≥ 15 contiguous years were available. Figure S.4.1 depicts examples of the latter. In Table S.4 for boxes A–C (8–12° N) all slopes except two are positive, and the majority significantly so ($p \leq 0.2$); over a period of 40 yr the median salinity increase estimated from the slopes was 0.11. In contrast, in the OMZ in and poleward of the D-boxes (15° N) negative values also occurred, especially at 15° N; here, the median salinity decrease from the regression slopes over 40 yr was 0.06. The observations support our earlier conclusion that there is little if any continuity of the OMZ with the region adjoining to the south. At 20–21° N salinity tended to increase. In boxes F2, G1, and G2 at 200–500 m, the median increase from the slopes was 0.0034 a^{-1} ($n = 5$), which corresponds to 0.13 over four decades.

BGD
10, 15455–15517, 2013

4.2 Oxygen

4.2.1 Seasonal variability of oxygen concentrations

Previous studies suggested either slightly better aeration during the SWM than in the NEM seasons in the upper few hundred meters of the OMZ (Naqvi, 1987; Naqvi et al., 1990; de Sousa et al., 1996) or did not find seasonal change (Morrison et al., 1999). Except for Naqvi (1987), the cited papers were based on only two cruises or (Morrison et al.) several cruises during one year and could not distinguish between seasonal and interannual changes.

With often four decades of observations for many boxes in our longitudinal band in hand, which include the above cited measurements by Naqvi and de Sousa, we treat climatology. The 150 m horizon is given short shrift because of the substantial interaction with surface waters (see Fig. 3). A methodological problem in interpreting our O_2 and NO_2^- data, besides the accuracy of the O_2 analyses, is the possible compounding of seasonal with decadal changes, which we disregarded for temperature and salinity. So, for comparisons among seasons we juxtapose similar years and focus on the NEM and SWM (December-March and June-September, respectively) in boxes D2 and F1 from the core of the OMZ. These boxes each offer a pair of regressions for the 200–500 m horizons for similar years in both seasons (Fig. 4, open symbols). Table 5 contains the statistics for all 18 seasonal data with ≥ 5 points (note some differences for periods between Fig. 4 and Table 5). As will be discussed in full in the next subsection, all slopes are negative, i.e., oxygen was decreasing with year and significantly so (at $p \leq 0.2$) in 7 out of 9 regression equations in Table 5 for Box D2.

The principal and surprising result about seasonality in the upper OMZ is that at all depths, the NEM and SI periods exhibit the highest O_2 values. All of the comparisons of medians in the 18 pairs in Table 4 are significant (at least at $p = 0.2$), and only in one is the SWM value the higher one of the pair. We are struck by the relative regularity of our data, although they are strongly biased upward as judged by the STOX observations. The similarity of the patterns (Fig. 4), especially the near-constant median O_2

BGD
10, 15455–15517, 2013

concentrations (Table 1) in spite of the great physical differences acting at the 200 m (diapycnal) and the 300 to 500 m levels (isopycnal) (Fig. 3), is truly noteworthy.

Regarding the causes of the seasonality, the high primary production of the SWM and the presumably enhanced vertical flux of particulate matter (see the sediment trap data at greater depths than our treatment near 15° N in Ramaswamy and Gaye, 2006) could be expected to lead to higher O_2 consumption and lower O_2 concentrations. Obviously, however, consumption cannot be the cause of the seasonal increase of O_2 during the NEM and SI periods, so the seasonal climatological progression of O_2 concentrations must principally be governed by advection. As noted in Sect. 4.1.2, at the 300 to 500 m levels the *T*-*S* diagram (Fig. 3) indicates isopycnal advection, most conspicuously during the FI period, with the transport direction during that time apparently from north to south in view of the increase of salinity to the north. While there is a tendency to a mild increase of O_2 in the far north (G-boxes, Table 1), the meridional gradients of the overall medians are smaller than would be expected from the seasonal ratios in Tables 4 and 5, so that O_2 must also be supplied laterally.

According to the model for the CAS domain of the central Arabian Sea by Resplandy et al. (2011, 2012), the vertical advection is most intensive in the upper OMZ (200–400 m), where the model similar to those in our observations yields increases of the O_2 values in the FI and NEM seasons and decreases in the late SI and SWM due to upward Ekman pumping. Further, Resplandy et al. (2012) stated for the NEM and SWM periods that the temporal O_2 change from vertical eddy-driven processes was 3–5 times that from biological consumption. The authors, however, estimated an annual amplitude of 6 µM of seasonal change in the upper OMZ to be "of the order of 5 %" of the annual mean O_2 concentrations of 40 µM. The range in the core and the lower OMZ was 1-3 µM of the concentrations of 20–40 µM (*op. cit.*, p. 5105). In contrast, we find the median and mean differences of 0.08 and 0.10 mL L^{-1}, respectively (~ 4.0 µM; range, 0.03–0.20 mL L^{-1}) of the 14 pairs "> SWM" in Table 4 to amount to 76 and 91 %, respectively, of the 0.105 and 0.11 mL L^{-1} (~ 4.5 µM) as median and mean of the 13 median O_2 concentrations for these boxes and depths (Table 1). The seasonality is

Discussion Paper | Discussion Paper | Discussion Paper | Discussion Paper |

BGD

10, 15455–15517, 2013

Oxygen minimum zone of the open Arabian Sea

K. Banse et al.

strong. Using a different model McCreary et al. (2013) likewise recognized the poleward horizontal advection and the role of the vertical advection of O_2.

In conclusion, in view of the strong advective processes, the apparently fairly steady maintenance of the annual balance between relatively rapid utilization and advection at the low prevailing oxygen concentrations is truly remarkable. Further, even when neglecting these newly evaluated historical data it is no longer advisable to base O_2 budgets for the central Arabian Sea on data from a single or even several cruises executed during only one season.

4.2.2 Four-decadal changes of O_2 in the upper OMZ

Neglecting the 150 m horizon in Table 5, the slopes of the 29 seasonal regressions – half being significant – are overwhelmingly negative, except in the northernmost boxes F2, G1, and G2. Three slopes at depth in F2 (20° N) are positive with very high significance, which proves that the decrease of O_2 in the bulk of our meridional swath is real rather than an artifact from an accuracy of the Winkler analyses increasing with time.

Table S.6 shows the computed annual slopes for O_2 concentrations on years for all boxes and depth ranges with ≥ 5 values each for 3 to 4 decades. Two remarkable results are: (1) the signs of the slopes for most depths in the southern boxes (A–C, 8–12° N) are positive, indicating an increasing trend in dissolved O_2 within the depth range examined (200–500 m). The median slope is 0.0024 $\mathrm{mL\,L^{-1}\,a^{-1}}$ ($n = 12$; 0.013 $\mathrm{mL\,L^{-1}\,a^{-1}}$ for the two significant slopes; [∼ 0.1 and 0.6 µM, respectively]). (2) Within the OMZ, in contrast, O_2 concentrations appear to have been decreasing, almost without exception, over four decades until the mentioned boxes F2, G1, and G2 (20-21° N) are reached. In boxes D1–F1 (the central OMZ after excluding the 150 m horizons in boxes E1, E2, and F1, cf. Table 1) the median slope is −0.00129 $\mathrm{mL\,L^{-1}\,a^{-1}}$ ($n =$ 21; 0.058 µM), while the median of the significant slopes is −0.00266 $\mathrm{mL\,L^{-1}\,a^{-1}}$ O_2 ($n = 13$; 0.120 µM). Multiplying the last rate by 40 yr, the predicted O_2 decrease would equal the median O_2 level of 0.11 $\mathrm{mL\,L^{-1}}$ between 200 and 500 m depth for the same period, which clearly was not the case because of O_2 advection. Further, Fig. 4 and Tables 5, 6, and S.6 imply the disappearance of O_2 during the current decades from most of the central Arabian Sea. Regrettably, the STOX probe has outdated this implication, which otherwise would have been sensational. In conclusion, the seasonal and decadal O_2 losses at depth appear to be largely replaced by advection, which, however, does not enter the OMZ directly from the south.

The same pattern as for the annual regressions of medians holds also for the medians of the within-season slopes on year in the OMZ boxes with ≥ 4 values each after omitting the 1960s, which weight the regressions perhaps unduly (Fig. 4, Table 6). Especially noticeable in the table is the number of statistically significant declines in Box D2, off Goa (for further details, see Supplement Sect. 6).

In summary, as with the O_2 concentrations, the rates of O_2 change on year over four decades in the central OMZ differ significantly between the two principal seasons, but O_2 does decline in both. The faster decreases are observed during the NEM with the higher O_2 concentrations, while the reverse holds for the SWM. For the two intermonsoon periods we have too few data to invite comments. The slopes for the two principal seasons change sign in the north.

4.3 Nitrite

The geochemical significance of the Arabian Sea principally rests on the presence or absence of denitrification and formation of N_2 (dinitrogen). Our NO_2^- observations for most depths and boxes extend from 1960–1965 to the beginning of the new century. Because we study this parameter as an indicator of active denitrification, the zero or near-zero values are considered only in passing. Note that once the denitrification threshold is crossed, NO_2^- is both produced and consumed. The accumulation is determined by several factors including the availability of substrates and the composition of the microbial community (Naqvi, 1991). An important pathway of NO_2^- consumption can be anammox, which combines NO_2^- and NH_4^+ (Dalsgaard et al., 2003, 2005; Kuypers et al., 2003; for the Arabian Sea see Nicholls et al., 2007, and Jensen et al., 2011).

BGD
10, 15455–15517, 2013

In the Arabian Sea, denitrification to N_2 rather than the anammox route was found by Ward et al. (2009, with earlier references; also Bulow et al., 2010) to be dominant. Lam et al. (2011), in contrast, stressed the anammox pathway leading to N_2 losses in OMZs. In this OMZ the highest NO_3^- deficit as well as the excess N_2 tend to coincide with the NO_2^- maximum, so the association of NO_2^- with active denitrification seems hard to argue against. While anammox is an autotrophic process, both NO_2^- and NH_4^+ are largely derived from the heterotrophic decomposition of organic matter and are therefore dependent on the supply of the latter. Ward (2013) reviewed new laboratory work showing the importance of the C : N ratio of the substrate, so we believe that the debate about which is the dominant path toward N_2 in the Arabian Sea may be close to solution.

4.3.1 Seasonality of nitrite concentrations

Previous research in the open Arabian Sea had suggested slightly higher NO_2^- values during the NEM than during the SWM periods (Naqvi et al., 1990; de Sousa et al., 1996). Assuming the NO_2^- concentration roughly reflects the strength of overall suboxic conditions, a more intense denitrification was inferred for the NEM. In contrast, Morrison et al. (1999) did not find consistent seasonal trends.

To avoid possible decadal bias, we compare seasons of similar intervals of years in Fig. 5 as we did with O_2. For the observations indicating active denitrification (> 0.5 µM), Table 7 lists the significant differences between seasons in median NO_2^- levels within depth ranges and boxes. As for O_2, the results may be taken as climatological medians at least for the horizons with more than four or five samples, in contrast to the work by those earlier authors who considered only one or two cruises. Note that we mainly deal with small differences between large numbers. As with O_2, the pattern is obscured when viewing the significant (Table 7) and non-significant pairs (not shown) together. The occurrences of higher NO_2^- during the NEM suggested here are in line with the cited earlier work.

4.3.2 Interannual variability of NO_2^-

In order to investigate the longer-term (interannual to decadal) changes in the intensity of suboxic conditions, we examined NO_2^- profiles at the location of GEOSECS sta. 416 (19°45′ N, 64°37′E, occupied in December 1977), visited by us nine times between 1992 and 2004. The site, placed in the southwestern corner of Box F1 (see Fig. 1), is close to the periphery of the suboxic zone, which makes it sensitive to changes in the volume and intensity of the reducing zone. Also it is well away from the continental margins and provides high-quality NO_2^- data going back to the 1970s.

The NO_2^- data exhibit large variability of the thickness of the secondary NO_2^- maximum, ranging from ~150 to ~500 m, and of the peak concentrations, varying between 0 and 4.6 µM (Fig. 6). However, since the observations were made in different seasons it is difficult to distinguish interannual from seasonal changes, or from those caused by smaller-scale spatio-temporal variability, which is fairly large in this region as demonstrated by the aforementioned results of the quasi-Lagrangian time-series study conducted around 21° N, 64° E (Sect. 3.1.d; Table 3: SK 121; Fig. S.3.1) in February 1997. Nevertheless, it would be reasonable to conclude that interannual changes may be quite substantial as well.

Most of the variability at this site seems to result from advection of PGW, which appears in Fig. S.3.1 and is a small but significant source of O_2 to the OMZ in the northwestern Arabian Sea (Codispoti et al., 2001). In the majority of our data from this location, the PGW salinity maximum was associated with a minimum in NO_2^-, whereas NO_2^- maxima often coincided with the salinity minimum overlying the PGW or just below the latter feature (Fig. 6). Moreover, despite the long period covered, the NO_2^- and salinity values within the approximate σ_θ range showed a significant inverse correlation ($r^2 = 0.36$, $p = 0.001$ for the slope, $n = 26$; Fig. 7). As is to be expected, the variability of salinity is matched with that of temperature (Fig. 8). For example, the most saline PGW core occurring in July 1995 was also the warmest, when the water column did not contain measurable NO_2^-, indicating the absence of denitrification (Fig. 6).

BGD
10, 15455–15517, 2013

Thus, while the observations demonstrate remarkable variations in the hydrographic structure and consequently in the redox environment, the changes – probably comprising both seasonal and interannual oscillations – are irregular and do not suggest a secular change in the redox environment over the past quarter-century. That is, the GEOSECS profile (showing some of the most intense reducing conditions recorded in the open Arabian Sea) is quite comparable with the most recent data (sta. AAS42, R/V *A. A. Siderenko*) collected during the same season (NEM of 2002).

At another site (15° N, 68° E, located on the eastern limit of Box D2), where reliable NO_2^- data go back to 1979 (to 1965 if we also include an R/V *Atlantis II* station at 14.03° N, 61.14° E) and which falls close to the zone of the most vigorous denitrification, the amplitude of variability (both seasonal and interannual) in NO_2^- is still quite large. Maximal concentrations observed during 18 visits ranged from 1.16 to 5.31 µM, while the thickness of the secondary NO_2^- maximum varied from < 100 m to > 300 m. Again, a consistent secular change in NO_2^- with time is not readily discernible.

4.3.3 Rates of decadal changes of nitrite

The slopes of NO_2^- concentrations of ≥ 0.5 and ≥ 1.5 µM on years for boxes and depths in the OMZ vary greatly and without an obvious pattern by either sign or value (Table S.7; representative plots in Fig. 5). In the two groupings of NO_2^- levels, positive slopes contribute 21 to a total of 29 in the first and 12 of 24 in the second group, respectively. Thus trends of increases in NO_2^- were more common than decreases. The distribution between seven positive and five negative significant slopes is without any pattern. The ranges (medians) for the positive and negative slopes are 0.0253 to 0.8363 (0.0498) and −0.0168 to −0.1035 (−0.0404) $\mu M\,a^{-1}$, respectively. The median increases and decreases correspond to 2.0 and 1.6 µM over four decades.

Few trends are obvious among the seasonal regressions on years (Table S.8). The positive slopes (increases of NO_2^-) are twice as frequent as the negative ones during the NEM and the SWM periods. Considering Tables S.7 and S.8 together, there is a suggestion for denitrification having undergone intensification during the four decades.

BGD
10, 15455–15517, 2013

To investigate decadal changes of NO_2^- in the OMZ in another way, the number of "zero values" (i.e., ≤ 0.2 µM), of ≥ 0.5 µM, and of ≥ 1.5 µM, each relative to the total number of NO_2^- values for a depth and box for 1985 and earlier, are compared with the data acquired since then (see Supplement, Sect. 7). The result is that denitrification increased after 1985 also as estimated in this manner.

In summary, more increases than decreases of NO_2^- were observed on the decadal scale among the regressions on year in spite of the great variability of the parameter, in contrast to the observations from the GEOECS site (Sect. 4.3.2). Similarly, the percentage of "zero values" increased in the eastern boxes in the second period, as did the ≥ 0.5 µM concentrations. For the ≥ 1.5 µM observations, denitrification likewise intensified in the three seasons with a sufficient number of data (NEM, SI, and SWM).

5 Implications of the results

5.1 Overview

The introduction into oceanography of the STOX sensor has opened a new era of reassessing all previous measurements of dissolved oxygen in the marine and freshwater bodies experiencing water-column oxygen depletion. We face the possible overthrow of long-standing results, unless a reasonably accurate conversion ratio for the historic data can be found, which we regard as unlikely. In any case, the STOX probe is another example from aquatic sciences of a new technology, rather than concepts, changing the field. Among new concepts in oceanography is the large investment of the last two or three decades into long-term time series observations without a specific hypothesis, which is so different from the canon of proper scientific conduct of hypothesis-driven original research (cf. Church et al., 2013).

We collate historic O_2 measurements – that may no longer be considered accurate enough – and NO_2^- data toward a time series, because we do not know of a reason why the temporal trends of O_2 would not hold in spite of the large bias shown by the STOX

BGD
10, 15455–15517, 2013

Oxygen minimum zone of the open Arabian Sea

K. Banse et al.

probe. In effect, we assume a bias with small enough variability that will not obliterate trends in O_2. Only time will tell whether our assumption was right, and two to three decades are required for a new, STOX-based time series. The regional and temporal coherence and consistencies of the O_2 distributions presented here, however, argue for the validity of using these seemingly outdated O_2 measurements.

Our NO_2^- values are not affected by the new nanomolar procedure for nitrite (Garside, 1982), because 4/5 of our samples are far above the lower limit of the traditional analytical method. In contrast, if the 1/5 of the near-zero records in our collation turn out to be too high by comparison with the new method, it would strengthen our point of the patchy occurrence of O_2 in the OMZ as preventing denitrification and supporting metazoan life.

The NO_2^- levels observed since 1933–1934 by every expedition looking for this species suggest that O_2 concentrations in the OMZ have been broadly nanomolar at least since that time. The presence of metazoans, however, which was noted at least that long, shows that the OMZ of the Arabian Sea not only was not sulfidic but was not functionally anoxic as stated for the tropical Pacific off South America by Thamdrup et al. (2012). Also, high NO_3^- concentrations were observed since the begin of measurement in the late 1950s. The disconnect of concentrations and temporal trends between salinity and O_2 in our meridional swath between the OMZ and the area adjoining to the south (Boxes A–C; Table 1; Sects. 4.1.3 and 4.2.2; Supplement Sect. S.1) shows that O_2 is advected into the OMZ from the southwest rather than directly from the south (cf. McCreary et al., 2013; Resplandy et al., 2012). It also implies that there has not been a general decrease in oxygen in the mesopelagic realm of the Arabian Sea as a whole as reported for the eastern Pacific (Stramma et al., 2010).

In addition, we describe strong seasonality of O_2 between 200 and 500 m depth with the SWM season showing significantly lower levels than found during the NEM. At 200 m and possibly at 250 m, the seasonal consumption is principally restored by eddies, while between 300 and 500 m new O_2 is advected horizontally. The O_2 loss is restored probably on an annual basis. Also, we observe statistically significant fast

BGD
10, 15455–15517, 2013

declines of O_2 between 15 and 20° N and increases at 20 and 21° N. The mean NO_2^- content in the OMZ probably increased especially after 1985.

5.2 Specific points for future work

5.2.1 Local time change and O_2 consumption

Any time series of O_2 in the sea determines the local (total) time change, which is the sum of the *x*, *y*, *z* components of advection and eddy diffusion plus the biological consumption (utilization). For direct measurement of the latter, enclosing of water and following the concentration changes during incubation are necessary, which is quite difficult because of the small rates of change in OMZ water and bottle effects on the enclosed organisms (for OMZ work, cf. Jayakumar et al., 2009; Stewart et al., 2012). However, knowing and understanding the regional distribution of seasonal change of biological consumption of O_2 and its variability is one of the holy grails of biogeochemistry of the sea.

We know of four computed estimates of O_2 consumption rate for OMZs, all made prior to the appearance of STOX and hence using too high O_2 concentrations, like we do for local time changes. The two earlier ones by Warren (1994) and Sarma (2002) determined the difference between the annual northward transport and the southward export of O_2 across 12° and 10° N, respectively, into the OMZ of the Arabian Sea and did not consider vertical or horizontal features. We mention only Warren (1994), who elaborated on a similar model by Olson et al. (1993) and estimated a consumption of 0.10 $mL\,L^{-1}\,a^{-1}$ for the depth interval of 200–1000 m. He estimated a possible error by about a factor of two. Both authors incorporated the coastal regions with their higher rates and the more intensive north-south water exchange than is to be expected in our central band. They also included the 500–1000 m depth interval (lower mesopelagial) where the O_2 consumption rate is reduced because of the oxidation of particles while sinking through the upper mesopelagial. Thus it would be difficult to guess a value parallel to the 250–300 m interval calculated by Resplandy et al. (2012) for the central

BGD
10, 15455–15517, 2013

Title Page
Abstract | Introduction
Conclusions | References
Tables | Figures
◀| |▶
◀ ▶
Back | Close
Full Screen / Esc
Printer-friendly Version
Interactive Discussion

Arabian Sea, but both Warren's (1994) and Sarma's (2002) ranges might have been of the order of a few times of 0.01 $mL\,L^{-1}\,a^{-1}$ (a few 10 $\mu L\,a^{-1}$)

Stramma et al. (2010) drew up O_2 budgets from the supply routes of water in a part of the OMZ of the eastern Pacific (3° N to 3° S; in the west to the date line, 200–700 m depth). They found a decrease in O_2 (total time change) of roughly 0.5 $\mu mol\,kg^{-1}\,a^{-1}$ and calculated an O_2 utilization rate of about 4 $\mu mol\,kg^{-1}\,a^{-1}$ (roughly 0.01 and 0.09 mL $L^{-1}\,a^{-1}$, respectively). As stated in Sect. 3.2.1, Resplandy et al. (2012) in their eddy-resolving model computed a median O_2 utilization rate of 2.8 $\mu mol\,L^{-1}\,a^{-1}$ (0.13 mL $L^{-1}\,a^{-1}$) for 250–300 m of depth for the central Arabian Sea. The rate declined with depth such that the median at 400 m was 0.85 $\mu mol\,L^{-1}\,a^{-1}$ (0.02 $mL\,L^{-1}\,a^{-1}$). Thus these two estimates of O_2 consumption vary from each other, which may not entirely be due to regional differences in primary production and food webs. Importantly, however, Resplandy et al. (2012) reported for the NEM and SWM that the amplitude of seasonal O_2 change from vertical eddy-driven advection was several times that from biological consumption (cf. their Fig. 6, CAS region), which is opposite to the result of Stramma et al. (2010). We cannot judge whether this gross divergence is due to the hydrographic settings of the two regions or the authors' approaches to the problem but note again that the O_2 utilization rate is a key parameter to know.

5.3 Decadal change of oxygen?

The origin of this paper during the late 1990s was a question about decadal variability in the OMZ, especially of O_2, and secular change, if any. The coherent south-north differences in the signs of significant slopes of the regressions of O_2 on year (Sect. 4.2.2; Table S.6) suggest an underlying reality, but do the decreases between 15° and 20° N (Fig. 4) signify a one-way street toward complete removal of O_2? A few STOX measurements especially in Box D2 off Goa appear as the most promising avenue to the answer, since is well studied and prone to low O_2. Because of the lack of O_2 measurements prior to the 1960s we cannot rule out the possibility that the decline of O_2 in the OMZ inferred from our data could be a part of the natural secular cycle.

5.4 Would global warming expand this OMZ?

Global change has reached the Arabian Sea. Since about 1960 the North Indian Ocean between about 200 and 500 m depth has warmed by up to 0.1 °C, most probably due to advection (Barnett et al., 2005). Based on an updated NODC data set (cf. Levitus, 2002), Harrison and Carson (2007: Fig. 6), using essentially the same database as Barnett et al. for the central open Arabian Sea, found an increase of very approximately 0.5°C for the period 1950-2000 at 100, 300, and 500 m depth.

In our view the answer to the question posed by the headline may depend on whether the present extent of the OMZ will remain as largely due to bottom-up processes, first of all due to circulation including O_2 advection at depth across the equator. In contrast, would the overall O_2 distribution in a changed climate depend more on the rate of O_2 consumption (utilization) by particulate and dissolved organic matter (POC, DOC), which is supplied from the euphotic zone by the top-down actions in the food web? Since according to the model by Resplandy et al. (2012) for the OMZ, advection within the basin is several times larger than consumption (see Sect. 4.2.1), should we worry about small biological changes and consumption?

Advected from outside of the model domain is the O_2-rich Subantarctic Mode Water of the South Indian Ocean. In a revisited cross-section along 32° S, Bindoff and McDougall (2000) observed an O_2 decrease of up to 0.2 mL L^{-1} near σ_θ of 27.2 kg m^{-3} (see our Fig. 3) between median dates of 1962 and 1987. The authors suggested a slowdown of circulation in the subtropical gyre as the cause, which allowed more time for O_2 consumption. Another repeat of the cross-section at 32° S in 2002, however, showed a reversal of the processes found for the period between the 1960s and 1987, suggesting a speeding up of the circulation of the subtropical gyre. Thus the sign points to variability rather than unidirectional global change, as stated by Bryden et al. (2003)

BGD
10, 15455–15517, 2013

for the region near 32° S, north of the formation region of the Mode Water and the O_2 source for the upper OMZ in the Arabian Sea.

If in contrast in the future in parts of the Arabian Sea consumption is to outrank advection (as presently in the eastern equatorial Pacific, Stramma et al., 2010), then the top-down effects of changes in zooplankton on the fraction of primary production that reaches the OMZ from above will become paramount (see Banse, 2013: 2.15.) This major problem is not merely figuratively sitting on top of the dependence on possible climate-related changes of circulation of regional, seasonal, and annual primary production.

Global warming will affect the seasons and alter the hydrography, as well as the community compositions, and hence the POC and DOC fluxes into the OMZ. The regime shift near Hawaii, a profound alteration in food web dynamics presumed to be due to quite small physical climate changes (Karl et al., 2001), is the warning by the proverbial writing on the wall: even when the physiological impact on phyto- or zooplankton species of as large an increase of 1 °C may be negligible, the community changes and ensuing biological impacts can at present not be foreseen from environmental information, let alone numerically predicted (for the demands on modeling see, e.g., Prowe et al., 2012). We do not even know the effect(s) on the biochemical processes determining the O_2 distribution from an adaptation to the STOX-era O_2 concentrations in the extant models.

In conclusion, for judging the impact of global change on the O_2 balance in the OMZ and on its vertical and horizontal extent, predictions of hydrographic changes and of O_2 consumption (utilization) must be of a useful accuracy. At least the latter may at present be out of reach.

Supplementary material related to this article is available online at http://www.biogeosciences-discuss.net/10/15455/2013/bgd-10-15455-2013-supplement.pdf.

BGD
10, 15455–15517, 2013

Acknowledgements. First of all we are indebted to the many anonymous colleagues who collected the samples, analyzed them in their laboratories, and largely deposited them in data centers. For additional observations we thank D. B. Olson in Miami and the late F. A. Schott in Kiel, as well as J. Hermann in Kiel. S. R. Emerson in Seattle and A. Körtzinger of Kiel and X anonymous reviewers made useful suggestions to the text. J. Pierson at the Horn Point Laboratory, Maryland, and H. Hadaway in Seattle helped with the designs of some figures. S. Tipple in Seattle arranged all the tables. K. Banse and J. R. Postel also wish to acknowledge the partial support by the US Office of Naval Research, grants No. N00014-97-1-0120 and N00014-04-1-0142. The printing of the paper was financed by K. Banse's TIAA/CREF account.

References

Anon.: Protocols for the Joint Global Ocean Flux Study (JGOFS) core measurements, Manual and Guides, 29, Intergov. Oceanogr. Comm./ Sci. Comm. Oceanic Res., UNESCO, Paris, 170 pp., 1994.

Artamonov, Yu. V.: The circulation and structure of water masses of the Arabian Sea based on synoptic surveys, in: The Mesoscale Structure of the Epipelagic Ecosystem of the Open Northern Arabian Sea, edited by: Banse, K. and Piontkovski, S. A., 12–46, Universities Press (India), Hyderabad, 2006.

Bange, H. W., Naqvi, S. W. A., and Codispoti, L. A.: The nitrogen cycle in the Arabian Sea, Progr. Oceanogr., 65, 145–158, 2005.

Banse, K.: Reflections about chance in my career, and on the top-down regulated world, Annu. Rev. Mar. Sci., 5, 2.1–2.19, doi:10.1146/annurev-marine-121211-172359, 2013.

Banse, K. and Postel, J. R.: Wintertime convection and ventilation of the upper pycnocline in the northernmost Arabian Sea, Indian Ocean Biogeochemical Processes and Ecological Variability, Geophys. Monogr. Ser., 185, 87–117, doi:10.1029/2008GM000704, 2009.

Barnett, T. P., Pierce, D. W., AchutaRao, K. M., Gleckler, P. J., Santer, B. D., Gregory, J. M., and Washington, W. M.: Penetration of human-induced warming into the world's ocean, Science, 309, 284–287, 2005.

Beal, L. M., Chereskin, T. K., Bryden, H. L., and Ffield, A.: Variable water properties, heat and salt fluxes in the Arabian Sea, between the onset and wane of the 1995 southwest monsoon, Deep-Sea Res. II, 50, 2049–2075, 2003.

Bendschneider, K. and Robinson, R. J.: A new spectrophotometric method for the determination of nitrite in seawater, J. Mar. Res., 11, 87–96, 1952.

Bianchi, D., Dunne, J. P., Sarmiento, J. L., and Galbraith, E. D.: Data-based estimates of suboxia, denitrification, and N_2O production in the ocean and their sensitivities to dissolved O_2, Global Biogeochem. Cy., 26, GB2009, doi:10.1029/2011GB004209, 2012.

Bindoff, N. L. and McDougall, T. J.: Decadal changes along an Indian Ocean section at 32° S and their interpretation, J. Phys. Oceanogr., 30, 1207–1222, 2000.

Bobko, N. I. and Rodionova, N. Yu.: Distribution of dissolved oxygen and biogenic elements in the northwestern Arabian Sea during February-March 1990, in: The Mesoscale Structure of the Epipelagic Ecosystem of the Open Northern Arabian Sea, edited by: Banse, K. and Piontkovski, S. A., 54–64, Universities Press (India), Hyderabad, 2006.

Böttger-Schnack, R.: Vertical structure of small metazoan plankton, especially non-calanoid copepods, I: Deep Arabian Sea, J. Plankt. Res., 18, 1073–1101, 1996.

Bryden, H. L., McDonagh, E. L., and King, B. A.: Changes in ocean water mass properties: Oscillations or trends?, Science, 300, 2086–2088, 2003.

Bulow, S. E., Rich, J. J., Naik, H. S., Pratihary, A. K., and Ward, B. B.: Denitrification exceeds anammox as a nitrogen loss pathway in the Arabian Sea oxygen minimum zone, Deep-Sea Res. I, 57, 384–393, doi:10.1016/j.dsr.2009.10.014, 2010.

Butler, M., Bollens, S. M., Burkhalter, B., Madin, L. P., and Horgan, E.: Mesopelagic fishes of the Arabian Sea: distribution, abundance and diet of *Chauliodus pammelas*, *Chauliodus sloani*, *Stomias affinis*, and *Stomias nebulosus*, Deep-Sea Res. II, 48, 1369–1383, 2001.

Chang, B. X., Devol, A. H., and Emerson, S. R.: Fixed nitrogen loss from the eastern tropical North Pacific and Arabian Sea oxygen deficient zones determined from measurements of N_2:Ar, Global Biogeochem. Cy., 26, GB3030, doi:10.1029/2011GB004207, 2012.

Chereskin, T. K., Wilson, W. D., and Beal, L. M.: The Ekman temperature and salt fluxes at 8°30′ N in the Arabian Sea during the 1995 southwest monsoon, Deep-Sea Res. II, 49, 1211–1230, 2002.

Church, M. J., Lomas, M. W., and Muller-Karger, F.: Sea change: charting the course for biogeochemical ocean time-series research in a new millennium, Deep-Sea Res. II, 93, 2–15, doi:10.1016/j.dsr2.2013.01.035, 2013.

Codispoti, L. A., Brandes, J. A., Christensen, J. P., Devol, A. H., Naqvi, S. W. A., Paerl, H. W., and Yoshinari, T.: The oceanic fixed nitrogen and nitrous oxide budgets: Moving targets as we enter the anthropocene?, Sci. Mar., 65 (Suppl. 2), 85–105, 2001.

Colborn, J. G.: The thermal structure of the Indian Ocean, International Indian Ocean Expedition Oceanogr. Monogr., 2, Univ. Press of Hawaii, Honolulu, 173 pp., 1975.

Cowie, G. L. and Levin, L. A.: Benthic biological and biogeochemical patterns and processes across an oxygen minimum zone (Pakistan margin, NE Arabian Sea), Deep-Sea Res. II, 56, 261–270, doi:10.1016/j.dsr2.2008.10.001, 2009.

Dalsgaard T., Canfield, T. E., Petersen, J., Thamdrup, B., and Gonzales, J. A.: N_2 production by the anammox reaction in the anoxic water column of Golfo Dulce, Costa Rica, Nature, 422, 606–608, 2003.

Dalsgaard T., Thamdrup, B., and Canfield, D. E.: Anaerobic ammonium oxidation (anammox) in the marine environment, Res. Microbiol., 156, 457–464, 2005.

de Sousa, S. N., Kumar, M. D., Sardessai, S., Sarma, V. V. S. S., and Shirodkar, P. V.: Seasonal variability in oxygen and nutrients in the central and eastern Arabian Sea, Current Sci., 71, 847–851, 1996.

Devol, A. H., Uhlenhopp, A. G., Naqvi, S. W. A., Brandes, J. A., Jayakumar, D. A., Naik, H., Gaurin, S., Codispoti, L. A., and Yoshinari, T.: Denitrification rates and excess nitrogen gas concentrations in the Arabian Sea oxygen deficient zone, Deep-Sea Res. I, 53, 1533–1547, doi:10.1016/j.dsr.2006.07.005, 2006.

Fabian, H., Koppelmann, R., and Weikert, H.: Full-depths zooplankton composition at two deep sites in the western and central Arabian Sea, Indian J. Mar. Sci., 34, 174–187, 2005.

Fischer, A. S., Weller, R. A., Rudnick, D. L., Eriksen, C. C., Lee, C. M., Brink, K. H., Fox, C. A., and Leben, R. R.: Mesoscale eddies, coastal upwelling, and the upper-ocean heat budget in the Arabian Sea, Deep-Sea Res. II, 49, 2231–2264, 2002.

Flagg, C. N. and Kim, H.-S.: Upper ocean currents in the northern Arabian Sea from shipboard ADCP measurements collected during the 1994-1996 U.S. JGOFS and ONR programs, Deep-Sea Res. II, 45, 1917–1959, 1998.

Garside, C.: A chemiluminescent technique for the determination of nanomolar concentrations of nitrate, nitrite, or nitrite alone in seawater, Mar. Chem., 11, 159–167, 1982.

Gilson, H. C.: The nitrogen cycle, Sci. Repts. John Murray Exp. 1933–34, 2, 21–81, 1937.

Hamner, W. M., Madin, L. P., Alldredge, A. L., Gilmer, R. W., and Hamner, P. O.: Underwater observations of gelatinous zooplankton: Sampling problems, feeding biology, and behavior, Limnol. Oceanogr., 20, 907–917, 1975.

Harrison, D. E., and Carson, M.: Is the World Ocean warming? Upper-ocean temperature trends: 1950–2000, J. Phys. Oceanogr., 37, 174–187, doi:10.1175/JPO3005.1, 2007.

BGD
10, 15455–15517, 2013

Howell, E. A., Doney, S. C., Fine, R. A., and Olson, D. B.: Geochemical estimates of denitrification in the Arabian Sea and the Bay of Bengal during WOCE, Geophys. Res. Lett., 24, 2549–2552, 1997.
Ignatyev, S. M.: Macrozooplankton in the Arabian Sea, in: The Mesoscale Structure of the Epipelagic Ecosystem of the Open Northern Arabian Sea, edited by: Banse, K. and Piontkovski, S. A., 151–161, Universities Press (India), Hyderabad, 2006.
Jayakumar, A., O'Mullan, G. D., Naqvi, S. W. A., and Ward, B. B.: Denitrifying bacterial community composition changes associated with stages of denitrification in oxygen minimum zones, Microb. Ecol., 58, 350–362, doi:10.1007/s00248-009-9487-y, 2009.
Jensen, M. M., Lam, P., Revsbech, N. P., Nagel, B., Gaye, B., Jetten, M. S. M., and Kuypers, M. M. M.: Intensive nitrogen loss over the Omani Shelf due to anammox coupled with dissimilatory nitrite reduction to ammonium, Int. Soc. Microb. Ecol. J., 5, 1660–1670, doi:10.1038/ismej.2011.44, 2011.
Karl, D. M., Bidigare, R. R., and Letelier, R. M.: Long-term changes in plankton community structure and productivity in the North Pacific Subtropical Gyre: the domain shift hypothesis, Deep-Sea Res. II, 48, 1449–1470, doi:10.1016/S0967-0645(00)00149-1, 2001.
Kim, H.-S., Flagg, C. N., and Howden, S. D.: Northern Arabian Sea variability from TOPEX/Poseidon altimetry data: an extension of the US JGOFS/ONR shipboard ADCP study, Deep-Sea Res. II, 48, 1069–1096, 2001.
Kuypers, M. M. M., Slickers, A. O., Lavik, G., Schmid, M., Jørgensen, B. B., Kuenen, J. G., Damsté, J. S. S., Strous, M., and Jetten, M. S. M.: Anaerobic ammonium oxidation by anammox bacteria in the Black Sea, Nature, 422, 608–611, 2003.
Lam, P., Jensen, M. M., Kock, A., Lettmann, K. A., Plancherel, Y., Lavik, G., Bange, H. W., and Kuypers, M. M. M.: Origin and fate of the secondary nitrite maximum in the Arabian Sea, Biogeosciences, 8, 1565–1577, doi:10.5194/bg-8-1565-2011, 2011.
Levitus, S. (Ed.): World Ocean Database 2001, NOAA Atlas NESDIS, 42–48, Nat. Oceanogr. Data Center, Ocean Climate Lab., Silver Springs, Maryland, 2002.
Lomas, M. W., and Lipschultz, F.: Forming the primary nitrite maximum: Nitrifiers or phytoplankton?, Limnol. Oceanogr., 51, 2453–2467, 2006.
Madhupratap, M., Gopalakrishnan, T. C., Haridas, P., and Nair, K. K. C.: Mesozooplankton biomass, composition and distribution in the Arabian Sea during the Fall Intermonsoon: implications of oxygen gradients, Deep-Sea Res. II, 48, 1345–1368, 2001.

BGD
10, 15455–15517, 2013

Mantoura, F. R. C., Law, C. S., Owens, N. J. P., Burkill, P. H., Malcolm, E., Woodward, S., Howland, R. J. M., and Llewellyn, C. A.: Nitrogen biogeochemical cycling in the northwestern Indian Ocean, Deep-Sea Res. II, 40, 651–671, 1993.

Maucha, R.: Hydrochemische Methoden in der Limnologie, Die Binnengewässer, 12, Schweizerbarth, Stuttgart, 173 pp., 1932.

McCreary Jr., J. P., Yu, Z., Hood, R. R., Vinaychandran, P. N., Furue, R., Ishida, A., and Richard, K. J.: Dynamics of the Indian-Ocean oxygen minimum zones, Progr. Oceanogr., 112–113, 15–37, doi:10.1016/j.pocean.2013.03.002, 2013.

Mincks, S. L., Bollens, S. M., Madin, L. P., Horgan, E., Butler, M., Kremer, P. M., and Craddock, J. E.: Distribution, abundance, and feeding ecology of decapods in the Arabian Sea, with implications for vertical flux, Deep-Sea Res. II, 47, 1475–1516, 2000.

Molinari, R. L., Festa, J. F., and Swallow, J. C.: Mixed layer and thermocline depth climatologies in the Western Indian Ocean, NOAA Technical Memorandum ERL AOML-64, 40 pp., 1986.

Morrison, J. M., Codispoti, L. A., Gaurin, S., Jones, B., Manghnani, V., and Zheng, Z.: Seasonal variation of hydrographic and nutrient fields during the US JGOFS Arabian Sea Process Study, Deep-Sea Res. II, 45, 2053–2101, 1998.

Morrison, J. M., Codispoti, L. A., Smith, S. L., Wishner, K., Flagg, C., Gardner, W. D., Gaurin, S., Naqvi, S. W. A., Manghnani, V., Prosperie, L., and Gundersen, J. S.: The oxygen minimum zone in the Arabian Sea during 1995, Deep-Sea Res. II, 46, 1903–1931, 1999.

Murray, C. N., Riley, J. P., and Wilson, T. R. S.: The solubility of oxygen in the Winkler reagents used for the determination of dissolved oxygen, Deep-Sea Res., 15, 237–238, 1968.

Naqvi, S. W. A.: Some aspects of the oxygen-deficient conditions and denitrification in the Arabian Sea, J. Mar. Res., 45, 1040–1072, 1987.

Naqvi, S. W. A.: Geographical extent of denitrification in the Arabian Sea in relation to some physical processes, Oceanol. Acta, 14, 281–290, 1991.

Naqvi, S. W. A. and Noronha, R. J.: Nitrous oxide in the Arabian Sea, Deep-Sea Res., 38, 871–890, 1991.

Naqvi, S. W. A. and Sen Gupta, R.: "NO", a useful tool for the estimation of nitrate deficits in the Arabian Sea, Deep-Sea Res., 32, 665–674, 1985.

Naqvi, S. W. A., Noronha, R. J., Somasundar, K., and Sen Gupta, R.: Seasonal changes in the denitrification regime of the Arabian Sea, Deep-Sea Res., 37, 593–611, 1990.

Discussion Paper | Discussion Paper | Discussion Paper | Discussion Paper |

Naqvi, S. W. A., Kumar, M. D, Narvekar, P. V., de Sousa, S. N., George, M. D., and D'Silva, C.: An intermediate nepheloid layer associated with high microbial metabolic rates and denitrification in the northwest Indian Ocean, J. Geophys. Res., 98 C, 16469–16479, 1993.

Naqvi, S. W. A., Sarma, V. V. S. S., and Jayakumar, D. A.: Carbon cycling in the northern Arabian Sea during the northeast monsoon: Significance of salps, Mar. Ecol.-Prog. Ser., 226, 35–44, 2002.

Naqvi, S. W. A., Bange, H. W., Gibb, S. W., Goyet, C., Hatton, A. D., and Upstill-Goddard, R. C.: Biogeochemical ocean-atmosphere transfers in the Arabian Sea, Progr. Oceanogr., 65, 116–144, 2005.

Naqvi, S. W A., Naik, H, Jayakumar, D. A., Shailaja, M. S., and Narvekar, P. V.: Seasonal oxygen deficiency over the western continental shelf of India, in: Past and Present Water Column Anoxia, edited by: Neretin, L. N., 195–224, NATO Science Ser., IV, 64, Springer, Dordrecht, The Netherlands, 2006.

Nicholls, J. C., Davies, C. A., and Trimmer, M., High-resolution profiles and nitrogen isotope tracing reveal a dominant source of nitrous oxide and multiple pathways of nitrogen gas formation in the central Arabian Sea, Limnol. Oceanogr., 52, 156–168, 2007.

Olson, D. B., Hitchcock, G. L., Fine, R. A., and Warren, B. A.: Maintenance of the low-oxygen layer in the central Arabian Sea, Deep-Sea Res. II, 40, 673–685, 1993.

Prakash, S., Balakrishnan Nair, T. M., Udaya Bhaskar, T. V. S., Prakash, P., and Gilbert, D.: Oxycline variability in the central Arabian Sea: An Argo-oxygen study, J. Sea Res., 71, 1–8, doi:10.1016/j.seares.2012.03.003, 2012.

Prasanna Kumar, S., Ramaiah, N., Mangesh Gauns, Sarma, V. V. S. S., Muraleedharan, P. M., Raghukumar, S., Dileep Kumar, M., and Madhupratap, M.: Physical forcing of biological productivity in the Northern Arabian Sea during the Northeast Monsoon, Deep-Sea Res. II, 48, 1115–1126, 2001.

Prowe, A. E. F., Pahlow, M., Dutkiewicz, S., Follows, M., and Oschlies, A.: Top-down control of marine phytoplankton diversity in a global ecosystem model, Progr. Oceanogr., 101, 1–13, doi:10.1016/j.pocean.2011.11.016, 2012.

Ramaswamy, V. and Gaye, B.: Regional variations in the fluxes of foraminifera carbonate, coccolithophorid carbonate and biogenic opal in the northern Indian Ocean, Deep-Sea Res. I, 53, 271–293, 2006.

Ramesh, K. V. and Krishnan, R.: Coupling of mixed layer processes and thermocline variations in the Arabian Sea, J. Geophys. Res. 110, C05005, doi:10.1029/2004JC002515, 2005.

BGD
10, 15455–15517, 2013

Oxygen minimum zone of the open Arabian Sea

K. Banse et al.

Ramesh Babu, V., Gangadhara Rao, L. V., and Varadachari, V. V. R.: Sea temperature variations in the northeastern Arabian Sea in relation to the southwest monsoon, in: Monsoon Dynamics, edited by: Lighthill, J. and Pearce, R. P., 481–540, Cambridge University Press, 1981.

Rao, R. R.: The observed variability of the cooling and deepening of the mixed layer in the central Arabian Sea during Monsoon-77, Mausam., 38, 43–48, 1987.

Resplandy, L., Lévy, M., Madec, G., Pous, S., Aumont, O., and Kumar, D.: Contribution of mesoscale processes to nutrient budgets in the Arabian Sea, J. Geophys. Res., 116, C11007, doi:10.1029/2011JC007006, 2011.

Resplandy, L., Lévy, M., Bopp, L., Echevin, V., Pous, S., Sarma, V. V. S. S., and Kumar, D.: Controlling factors of the oxygen balance in the Arabian Sea's OMZ, Biogeosciences, 9, 5095–5109, doi:10.5194/bg-9-5095-2012, 2012.

Revsbech, N. P., Larsen, L. H., Gundersen, J., Dalsgaard, T., Ulloa, O., and Thamdrup, B.: Determination of ultra-low oxygen concentrations in oxygen minimum zones by the STOX sensor, Limnol. Oceanogr. Methods, 7, 371–381, 2009.

Saltzman, J. and Wishner, K. F.: Zooplankton ecology in the eastern tropical Pacific oxygen minimum zone above a seamount, I. General trends, Deep-Sea Res. I, 44, 907–930, 1997.

Sarma, V. V. S. S.: An evaluation of physical and biogeochemical processes regulating perennial suboxic conditions in the water column of the Arabian Sea, Global Biogeochem. Cy., 16, 1099, doi:10.1029/2002GB001920, 2002.

Schenau, S. J., Reichart, G. J., and De Lange, G. J.: Oxygen minimum zone controlled Mn redistribution in Arabian Sea sediments during the late Quaternary, Paleoceanography, 17, 1058, doi:10.1029/2000PA000621, 2002.

Sen Gupta, R. and Naqvi, S. W. A.: Chemical oceanography of the Indian Ocean, north of the equator, Deep-Sea Res., 31, 671–706, 1984.

Sen Gupta, R., Rajagopal, M. D., and Qasim, S. Z.: Relationship between dissolved oxygen and nutrients in the north-western Indian Ocean, Indian J. Mar. Sci., 5, 201–211, 1976.

Shankar, D., Vinayachandran, P. N., and Unnikrishnan, A. S.: The monsoon currents in the north Indian Ocean, Progr. Oceanogr., 52, 63–120, 2002.

Smith, S. L. and Madhupratap, M.: Mesozooplankton of the Arabian Sea: Patterns influenced by seasons, upwelling, and oxygen concentrations, Progr. Oceanogr., 65, 214–239, doi:10.1016/j.pocean.2005.03.007, 2005.

BGD
10, 15455–15517, 2013

Oxygen minimum zone of the open Arabian Sea

K. Banse et al.

Somasundar, K. and Naqvi, S. W. A.: On the renewal of the denitrifying layer in the Arabian Sea, Oceanol. Acta, 11, 167–172, 1988.
Staubwasser, M., Sirocko, F., Grootes, P. M., and Erlenkeuser, H.: South asian monsoon climate change and radiocarbon in the Arabian Sea during early and middle Holocene, Paleoceanography, 17, 1063, doi:10.1029/2000PA000608, 2002.
Stewart, F. J., Dalsgaard, T., Young, C. R., Thamdrup, B., Revsbech, N. P., Ulloa, O., Canfield, D. E., and DeLong, E. F.: Experimental incubations elicit profound changes in community transcription in OMZ bacterioplankton, PloS On3, 7, e37118, doi:10.1371/journal.pone.0037118, 2012.
Stramma, L., Brandt, P., Schott, F., Quadfasel, D., and Fischer, J.: Winter and summer monsoon water mass, heat and freshwater transport changes in the Arabian Sea near 8° N, Deep-Sea Res. II, 49, 1173–1195, 2002.
Stramma, L., Johnson, G. C., Firing, E., and Schmidtko, S.: Eastern Pacific oxygen minimum zones: Supply paths and multidecadal changes, J. Geophys. Res., 115, C09011, doi:10.1029/2009JC005976, 2010.
Thamban, M., Kawahata, H., and Purnachandra Rao, V.: Indian summer monsoon variability during the Holocene as recorded in sediments of the Arabian Sea: timing and implications, J. Oceanogr., 63, 1009–1020, 2007.
Thamdrup, B., Dalsgaard, T., and Revsbech, N. P.: Widespread functional anoxia in the oxygen minimum zone of the Eastern South Pacific, Deep-Sea Res. I, 65, 36–45, doi:10.1016/j.dsr.2012.03.001, 2012.
Ulloa, O., Canfield, D. E., DeLong, E. F., Letelier, R. M., and Stewart, F. J.: Microbial oceanography of anoxic oxygen minimum zones, P. Acad. Nat. Sci., 109, 15996–16003, doi:10.1073/pnas.1205009109, 2012.
Vinogradov, M. E.: Vertical distribution of the oceanic zooplankton, Moscow: Nauka, 318 pp., 1968 (in Russian; Engl. transl. by Israel Progr. Scient. Transl., Jerusalem, 1970, 339 pp.).
Vinogradov, M. E., and Voronina, N. M.: Influence of the oxygen deficit on the distribution of plankton in the Arabian Sea, Deep-Sea Res., 9, 523-530, 1962 (transl. of the Russian original in Okeanologiya, 1, 1961).
Vinogradov, M. E., Shushkina, E. A., Gorbunov, A. Y., and Shashkov, N. L.: Vertical distribution of the macro- and mesoplankton in the region of the Costa Rica Dome, Oceanology, 31, 559–556, 1991 (Russian original in Okeanologiya, 31, 1990).

BGD
10, 15455–15517, 2013
Oxygen minimum zone of the open Arabian Sea
K. Banse et al.

von Rad, U., Schulz, H., and Sonne 90 Scientific Party: Sampling the oxygen minimum zone off Pakistan: glacial-interglacial variations of anoxia and productivity (preliminary results, Sonne 90 cruise), Mar. Geol., 125, 7–19, 1995.

von Rad, U., Schaaf, M., Michels, K. H., Schultz, H., Berger, W. H., and Sirocko, F.: A 5000-yr record of climate change in varved sediments from the oxygen minimum zone off Pakistan, northeastern Arabian Sea, Quaternary Res., 51, 39–53, 1999.

Ward, B. B.: Nitrification in marine systems, in: Nitrogen in the Marine Environment, 2nd ed., edited by: Capone, D. G., Bronk, D. A., Mulholland, M. R., and Carpenter, E. J., Elsevier, 199–261 (Electronic book, ISBN 9780123725226), 2008.

Ward, B. B.: How nitrogen is lost, Science, 341, 352–353, doi:10.1126/science.1240314, 2013.

Ward, B. B., Tuit, C. B., Jayakumar, A., Rich, J. J., Moffett, J., and Naqvi, S. W. A.: Organic carbon, and not copper, controls denitrification in oxygen minimum zones of the ocean, Deep-Sea Res. I, 55, 1672-1683, 2008.

Ward, B. B., Devol, A. H., Rich, J. J., Chang, B. X., Bulow, S. E., Naik, H., Pratihary, A., and Jayakumar, A.: Denitrification as the dominant nitrogen loss process in the Arabian Sea, Nature, 461, 78–81, doi:10.1038/nature08276, 2009.

Warren, B. A.: Transindian hydrographic section at Lat. 18° S: Property distributions and circulation in the South Indian Ocean, Deep-Sea Res., 28, 759–788, 1981.

Warren, B. A.: Context of the suboxic layer in the Arabian Sea, Proc. Indian Acad. Sci. (Earth Planet. Sci.), 103, 301–314, 1994.

Weller, R. A., Fischer, A. S., Rudnick, D. L., Eriksen, C. C., Dickey, T. D., Marra, J., Fox, C., and Leben, R.: Moored observations of upper-ocean response to the monsoons in the Arabian Sea during 1994–1995, Deep-Sea Res. II, 49, 2195–2230, 2002.

Wiggert, J. D., Hood, R. R., Banse, K., and Kindle, J. C.: Monsoon-driven biogeochemical processes in the Arabian Sea, Progr. Oceanogr., 65, 176–213, doi:10.1016/j.pocean.2005.03.008, 2005.

Wishner, K. F., Gowing, M. M., and Gelfman, C.: Mesozooplankton biomass in the upper 1000 m in the Arabian Sea: overall seasonal and geographic patterns, and relationship to oxygen gradients, Deep-Sea Res. II, 45, 2405–2432, 1998.

Wishner, K. F., Gelfman, C., Gowing, M. M., Outram, D. M., Rapien, M., and Williams, R. L.: Vertical zonation and distributions of calanoid copepods through the lower oxycline of the Arabian Sea oxygen minimum zone, Progr. Oceanogr., 78, 163–191, doi:10.1016/j.pocean.2008.03.001, 2008.

Wong, G. T. F.: Removal of nitrite interference in the Winkler determination of dissolved oxygen, Mar. Chem., 130–131, 28–32, doi:10.1016/j.marchem.2011.11.003, 2011.

Wyrtki, K.: Oceanographic Atlas of the International Indian Ocean Expedition, National Science Foundation, Washington, DC, 529 pp., 1971.

BGD

10, 15455–15517, 2013

Oxygen minimum zone of the open Arabian Sea

K. Banse et al.

Table 1. Median O_2 concentrations (mL L^{-1}) for all boxes near the indicated depths (number of values in parentheses; data in Table S.1.b). One-sided p for O_2 difference between adjoining medians: * ≤ 0.20; ** ≤ 0.10; *** ≤ 0.05); blank, non-significant.[1]

Box	150 m	200 m	300 m	400 m	500 m
A1 + A2	0.77 (3)	0.99 (5)	1.21 (4)	0.92 (1)	0.96 (4)
	***	***	**		**
B1	0.24 (8)	*0.30 (13)	***0.72 (7)	0.68 (8)	**0.48 (9)
		*	**	**	***
C1	0.39 (2)	0.27 (6)	0.36 (3)	0.44 (3)	0.36 (6)
		**		***	***
D1	0.07 (9)	0.10 (12)	0.04 (9)	**0.09 (11)	*0.13 (13)
	***		***		
E1	0.22 (10)	**0.12 (9)	*0.10 (7)	0.09 (8)	**0.13 (9)
			*	*	**
F1	0.27 (25)	***0.14 (23)	0.10 (17)	0.09 (19)	0.10 (16)
				*	*
G1	0.30 (19)	***0.13 (15)	0.15 (12)	0.15 (12)	***0.10 (7)
B2	0.16 (10)	**0.24 (13)	***0.67 (11)	*0.59 (9)	*0.54 (12)
	**		**		**
C2	0.47 (3)	0.37 (5)	*0.25 (2)	1.04 (2)	0.34 (4)
	***	***	***	***	***
D2	0.07 (17)	0.06 (23)	0.07 (20)	0.11 (25)	0.12 (26)
	***				
E2	0.19 (10)	**0.04 (5)	0.13 (4)	0.09 (5)	***0.11 (9)
F2	0.13 (10)	0.09 (7)	0.07 (8)	0.06 (8)	0.10 (11)
	*		**	***	***
G2	0.43 (9)	***0.08 (9)	***0.05 (4)	0.04 (5)	0.05 (4)

[1] The significance of differences is determined between pairs of medians, on-line (within a box) and between-lines (between adjoining boxes), and is expressed by asterisks or blanks (for non-significance). For example, horizontally for B1 the asterisk preceding 0.30 at 200 m states significance at $p < 0.20$ of the difference between the medians of 0.24 at 150 m and 0.30 at 200 m. Vertically, in contrast, the 3 asterisks beneath 0.77 at 150 m state significance at $p < 0.05$ of the difference between the medians of 0.77 for (A1 + A2) and 0.24 for B1.

Table 2. Median NO_2^- concentrations (µM) for all boxes near the indicated depths (number of values in parentheses; data in Table S.1.b). One-sided p for NO_2^- difference between adjoining medians in boxes D–G: * ≤ 0.20; ** ≤ 0.10; *** ≤ 0.05; blank, non-significant (see also footnote in Table 1).

Box	150 m		200 m		300 m		400 m		500 m
A1 + A2	0.01 (10)		0.01 (10)		0.01 (7)		0.01 (7)		0.01 (7)
B1	0.02 (14)		0.01 (18)		0.00 (15)		0.00 (14)		0.00 (14)
C1	0.03 (12)		0.04 (18)		0.00 (11)		0.00 (13)		0.00 (12)
D1	0.13 (30)		0.81 (34)	*	1.17 (32)	***	0.00 (29)	***	0.00 (29)
	***				***		***		***
E1	0.02 (15)	***	0.40 (16)	**	2.86 (15)	***	1.32 (16)	***	0.04 (11)
	*				***				***
F1	0.04 (36)	***	0.14 (45)	**	1.36 (41)	**	1.37 (38)	***	0.43 (37)
	*				***		**		
G1	0.03 (30)	***	0.23 (34)		0.53 (31)		0.75 (32)	**	0.54 (28)
B2	0.02 (9)		0.00 (9)		0.00 (8)		0.00 (4)		0.00 (5)
C2	0.00 (4)		0.00 (6)		0.00 (5)		0.01 (4)		0.00 (6)
D2	2.00 (35)	***	2.83 (40)	***	1.22 (38)	***	0.01 (36)	***	0.00 (35)
	***				***		***		***
E2	0.08 (16)	***	2.53 (18)		2.74 (15)	***	1.28 (17)	***	0.06 (17)
			**				**		**
F2	0.07 (6)	***	1.74 (9)	***	2.82 (9)	***	1.44 (7)	**	0.95 (5)
			*						*
G2	0.04 (12)	***	0.46 (14)	***	2.67 (14)	***	1.98 (14)	***	1.26 (13)

BGD
10, 15455–15517, 2013
Oxygen minimum zone of the open Arabian Sea
K. Banse et al.

Table 3. Mean values with S.D. on drift stations (number of samples in parentheses).

	150 m	200 m	300 m	400 m	500 m
SK 99:17, 19–21 February 1995, west of D1* (O_2 automated end point)					
T (°C)	18.95 ± 0.50 (7)	16.63 ± 0.27 (7)	13.96 ± 0.09 (8)	12.86 ± 0.07 (6)	12.18 ± 0.09 (5)
S	35.69 ± 0.04 (7)	35.73 ± 0.01 (7)	35.64 ± 0.01 (8)	35.61 ± 0.01 (6)	35.60 ± 0.01 (5)
O_2 (mL L^{-1})	0.30 ± 0.065 (6)	0.05 ± 0.03 (4)	0.05 ± 0.03 (6)	0.08 ± 0.08 (7)	0.09 ± 0.09 (7)
NO_2^- (µM)	0.06 ± 0.11 (7)	0.90 ± 0.85 (6)	2.36 ± 0.47 (7)	0.05 ± 0.08 (5)	0 (5)
ME 32/3:243-252, 10–18 May 1995, E1** (O_2 automated end point); T and S include sta. 240 of 9 May					
T (°C)	20.94 ± 0.45 (9)	17.54 ± 0.13 (11)	15.10 ± 0.27 (12)	13.57 ± 0.10 (11)	11.49 ± 0.10 (11)
S	35.94 ± 0.13 (9)	35.62 ± 0.02 (11)	35.82 ± 0.06 (12)	35.76 ± 0.02 (11)	35.57 ± 0.01 (11)
O_2 (mL L^{-1})	0.31 ± 0.31 (11)	0.08 ± 0.015 (10)	0.09 ± 0.02 (5)	0.08 ± 0.02 (7)	–
NO_2^- (µM)	0.04 ± 0.02 (13)	3.54 ± 0.77 (10)	2.86 ± 0.82 (4)	2.36 ± 0.58 (7)	–
SK 121:8, 10–22 February 1997, western edge of G1*** (O_2 visual end point)					
T (°C)	20.23 ± 0.57 (24)	18.08 ± 0.25 (20)	15.78 ± 0.38 (23)	14.05 ± 0.26 (23)	13.06 ± 0.19 (23)
S	35.99 ± 0.06 (22)	35.89 ± 0.06 (18	36.03 ± 0.07 (23)	35.85 ± 0.05 (23)	35.77 ± 0.03 (23)
O_2 (mL L^{-1})	0.25 ± 0.20 (27)	0.04 ± 0.04 (24)	0.06 ± 0.04 (26)	0.05 ± 0.04 (25)	0.06 ± 0.07 (27)
NO_2^- (µM)	0.03 ± 0.06 (27)	0.57 ± 0.79 (24)	0.38 ± 0.86 (27)	0.85 ± 0.99 (27)	0.34 ± 0.60 (27)

* Drifting over a range of about 1 km.
* Drifting over a range of about 2 km.
** Drifting over a range of about 45 km, see Naqvi et al. (2002: Fig. 1) and Supplement Fig. S.3.1.

BGD
10, 15455–15517, 2013
Oxygen minimum zone of the open Arabian Sea
K. Banse et al.

Table 4. Significant seasonal differences in median O_2 concentrations ($mL\,L^{-1}$) in the OMZ for boxes and depths with ≥ 2 values during similar periods. One-sided *p*: *, ≤ 0.20; **, ≤ 0.10; ***, ≤ 0.05. See Fig. 3 for names of seasons and months.

Box	Depth (m)	Year (add 1900)	Season	*p*	$n^{\dagger}$
D1	200	'63–'96	SWM > SI	0.20*	(0.12/0.00; 8/3)
	400	'94–'96	SI > SWM	0.10**	(0.20/0.09; 2/3)
	500	'94–'96	SI > SWM	0.10**	(0.24/0.13; 2/3)
F1	400	'87–'104	NEM > SWM	0.01***	(0.13/0.08; 9/5)
	500	'87–'104	NEM > SWM	0.01***	(0.12/0.08; 8/4)
	200	'90–'96	SI > SWM	0.10**	(0.20/0.01; 4/3)
	300	'90–'96	SI > SWM	0.20*	(0.17/0.09; 3/3)
G1	300	'88–'94	NEM > SI	0.10**	(0.19/0.15; 4/4)
	400	'87–'97	NEM > SWM	0.20*	(0.15/0.04; 4/2)
	200	'88–'90	SI > NEM	0.05***	(0.29/0.13; 3/3)
	400	'88–'90	SI > NEM	0.10**	(0.21/0.16; 2/3)
	200	'87–'96	SI > SWM	0.05***	(0.27/0.07; 3/3)
	400	'87–'96	SI > SWM	0.05***††	(0.21/0.04; 2/2)
D2	200	'87–'98	NEM > SWM	0.05***	(0.08/0.03; 10/5)
	300	'87–'98	NEM > SWM	0.10**	(0.08/0.05; 8/4)
	400	'83–'98	NEM > SWM	0.10**	(0.11/0.05; 9/6)
	400	'80–'96	FI > SWM	0.10**	(0.20/0.05; 4/6)
	500	'80–'96	FI > SWM	0.05***	(0.19/0.11; 3/7)

† Median concentrations and numbers of samples for the two seasons.
†† Estimated *p*.

BGD
10, 15455–15517, 2013

Table 5. Seasonal regressions of O_2 on year in OMZ with slopes and medians with $n \geq 5$ (p of slope: * ≤ 0.20; ** ≤ 0.10; *** ≤ 0.05; n number of values; S.E.: Standard Error of regression). See Fig. 3 for names and length of seasons.

Box	Depth (m)	Season	Year (add 1900)	Median ($mL\,L^{-1}$)	Slope ($mL\,L^{-1}\,a^{-1}$)	p	n	S.E.
D1	150	SWM	'63–'104	0.15	−0.0017	0.70	5	0.140
	200	SWM	'63–'104	0.12	−0.0019	0.19*	8	0.069
	300	SWM	'63–'104	0.04	−0.0025	0.25	7	0.095
	400	SWM	'63–'104	0.09	−0.0005	0.57	7	0.032
	500	SWM	'63–'104	0.13	−0.0008	0.42	9	0.041
F1	150	NEM	'77–'102	0.32	−0.0033	0.89	14	0.458
	200	NEM	'88–'102	0.15	−0.0091	0.19*	12	0.090
	300	NEM	'88–'102	0.10	−0.0062	0.12*	9	0.045
	400	NEM	'88–'102	0.13	−0.0056	0.22	9	0.054
	500	NEM	'88–'102	0.12	−0.0047	0.17*	8	0.041
	150	SI	'90–'94	0.34	−0.0338	0.40	5	0.198
	150	SWM	'63–'104	0.10	−0.0001	0.99	5	0.108
	200	SWM	'63–'104	0.04	−0.0009	0.69	5	0.068
	400	SWM	'63–'104	0.09	−0.0020	0.05**	5	0.023
	500	SWM	'63–'104	0.09	−0.0014	0.07**	6	0.021
G1	150	NEM	'65–'97	0.28	0.0086	0.29	10	0.190
	200	NEM	'65–'97	0.08	0.0015	0.73	5	0.100
	300	NEM	'65–'97	0.16	0.0044	0.43	6	0.125
	400	NEM	'65–'97	0.15	0.0014	0.61	5	0.058
	300	SI	'94–'102	0.15	−0.0056	0.59	5	0.095
	150	FI	'63–'88	0.28	−0.0017	0.81	5	0.188

Table 5. Continued.

Box	Depth (m)	Season	Year (add 1900)	Median ($mL\,L^{-1}$)	Slope ($mL\,L^{-1}\,a^{-1}$)	*p*	*n*	S.E.
D2	150	NEM	'88–'98	0.06	−0.0037	0.02***	7	0.012
	200	NEM	'88–'98	0.08	−0.0015	0.59	10	0.037
	300	NEM	'88–'98	0.08	−0.0041	0.13*	8	0.027
	400	NEM	'77–'98	0.11	−0.0036	0.07**	10	0.036
	500	NEM	'77–'98	0.15	−0.0008	0.72	9	0.043
	150	SWM	'63–'104	0.07	−0.0056	0.58	7	0.325
	200	SWM	'63–'104	0.04	−0.0016	0.09**	9	0.035
	300	SWM	'63–'104	0.04	−0.0025	0.01***	7	0.014
	400	SWM	'63–'104	0.06	−0.0037	0.10**	8	0.063
	500	SWM	'63–'104	0.09	−0.0022	0.16*	11	0.065
E2	150	NEM	'63–'92	0.36	0.0090	0.34	5	0.063
	500	NEM	'63–'92	0.11	0.0020	0.59	5	0.079
F2	150	NEM	'65–'88	0.15	0.0003	0.96	7	0.209
	200	NEM	'65–'88	0.08	0.0014	0.26	6	0.029
	300	NEM	'65–'88	0.06	0.0048	0.02***	5	0.022
	400	NEM	'65–'88	0.06	0.0046	0.05***	6	0.045
	500	NEM	'65–'88	0.11	0.0038	0.01***	8	0.029
G2	150	NEM	'65–'92	0.43	−0.0200	0.21	5	0.280
	200	NEM	'65–'77	0.08	0.0090	0.12*	5	0.055

BGD
10, 15455–15517, 2013

Table 6. Medians with slopes and intercepts of seasonal regressions of O_2 on year in the OMZ without 1960s with ≥ 4 values during similar periods. *p*: * ≤ 0.20; ** ≤ 0.10; *** ≤ 0.05; *n* number of values; S.E. Standard Error of regression. See Fig. 3 for names of seasons and months.

Box	Depth (m)	Season	Year (add 1900)	Median ($mL\,L^{-1}$)	Slope ($mL\,L^{-1}\,a^{-1}$)	*p*	*n*	Interc. ($mL\,L^{-1}$)	S.E.
D2	200	NEM	’88–’98	0.08	−0.0015	0.58	10	3.1	0.037
	200	SWM	’87–’104	0.03	−0.0039	0.19*	7	7.8	0.037
	300	NEM	’88–’98	0.08	−0.0041	0.13*	8	8.2	0.027
	300	SWM	’87–’104	0.04	−0.0026	0.07**	6	5.2	0.015
	400	NEM	’88–’98	0.11	−0.0071	0.03***	9	14.3	0.033
	400	SWM	’86–’104	0.05	−0.0087	0.05***	6	17.4	0.055
	400	FI	’80–’96	0.20	−0.0134	0.12*	4	26.9	0.069
	500	NEM	’88–’98	0.15	−0.0065	0.05***	8	13.1	0.032
	500	SWM	’86–’104	0.09	−0.0052	0.05***	8	10.5	0.037
F1	200	NEM	’88–’102	0.15	−0.0091	0.19*	12	18.3	0.090
	200	SI	’90–’96	0.20	−0.0131	0.23	4	26.4	0.040
	200	SWM	’95–’104	0.03	−0.0025	0.84	4	5.0	0.083
	300	NEM	’88–’102	0.10	−0.0062	0.12*	9	12.4	0.045
	300	SWM	’95–’104	0.07	−0.0140	0.37	4	28.1	0.092
	400	NEM	’88–’102	0.13	−0.0056	0.22	9	11.2	0.054
	400	SWM	’87–’104	0.08	−0.0043	0.08**	5	8.6	0.020
	500	NEM	’88–’102	0.12	−0.0047	0.17*	8	9.5	0.041
	500	SWM	’87–’104	0.08	−0.0019	0.45	4	3.8	0.024
G1	300	SI	’90–’94	0.15	−0.0292	0.41	4	58.3	0.098

BGD
10, 15455–15517, 2013

Oxygen minimum zone of the open Arabian Sea

K. Banse et al.

Table 7. Significant seasonal differences in median NO_2^- concentrations with $n \geq 2$ (> 0.5 µM) in the OMZ for boxes and depths during similar periods. One-sided p: with ≥ 2 values, * ≤ 0.20; ** ≤ 0.10; *** ≤ 0.05. See Fig. 3 for names of seasons and months.

Box	Depth (m)	Years (add 1900)	Seasons	p	n[†]
D1	200	'95–'96	SWM > NEM	0.20*	(4.84/3.44; 3/5)
E1	300	'64–'96	SWM > SI	0.20*	(3.23/2.82; 3/2)
F1	300	'90	NEM > SI	0.20*	(1.71/1.60; 5/2)
	400	'90–'96	NEM > SI	0.01***	(1.66/1.05; 10/4)
	200	'83–'95	SWM > SI	0.10**	(3.90/2.24; 4/4)
	200	'87–'95	SWM > NEM	0.10**	(3.90/2.10; 4/8)
	400	'87–'96	SWM > SI	0.20*	(1.66/1.05; 6/4)
G1	200	'83–'95	NEM > SI	0.05***	(3.71/1.18; 5/3)
	200	'60–'95	NEM > FI	0.20*	(3.50/1.60; 6/3)
	200	'83–'95	SWM > SI	0.10**	(3.04/1.18; 2/3)
	500	'60–'95	FI > SWM	0.10**	(1.30/0.78; 2/4)
D2	150	'83–'96	FI > SWM	0.20*	(5.31/2.00; 3/10)
E2	200	'60–'95	NEM > SI	0.10**	(3.36/2.58; 7/3)
	200	'87–'95	NEM > SWM	0.20*	(3.49/2.01; 6/4)
	300	'87–'88	SWM > NEM	0.20*	(3.22/2.53; 2/4)

[†] Median concentrations and number of values for the two seasons.

BGD
10, 15455–15517, 2013

K. Banse et al.

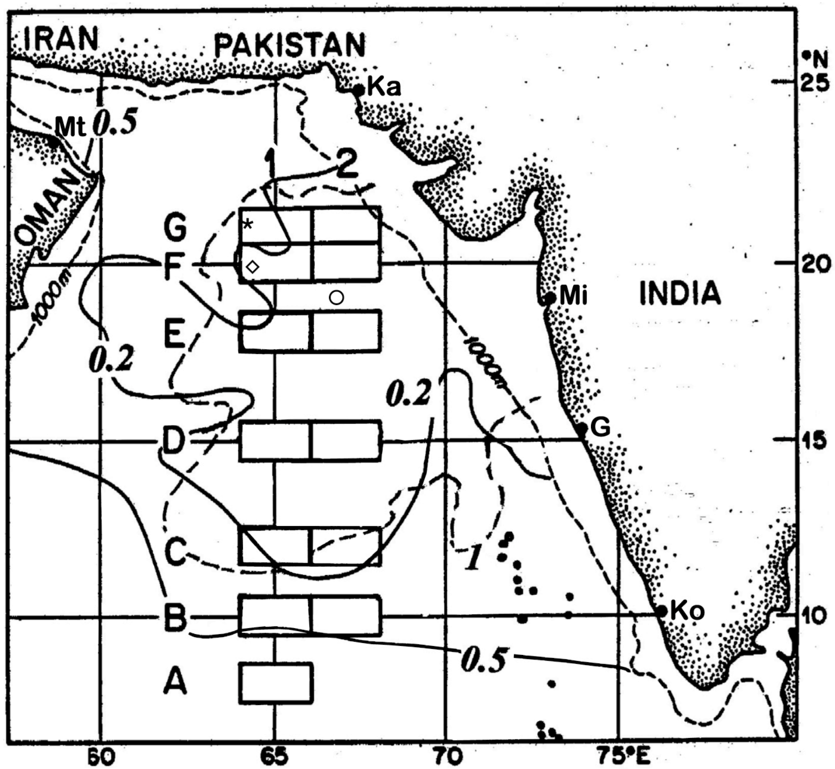

Fig. 1. Distribution of the boxes (left series, "1", right series, "2") with outlines of O_2 concentration ($mL\,L^{-1}$) at 200 m (from Wyrtki, 1971) and the nitrite maximum (circumscribed by the 1 µM contour) in the OMZ (from Naqvi, 1991). Circle, position of drift station shown in Fig. 2; diamond, position of GEOSECS sta. 416; asterisk, position of drift station depicted in Supplement Fig. S.3.1; G, Goa; Ka, Karachi; Ko, Kochi (former Cochin); Mi, Mumbai (former Bombay); Mt, Muscat.

BGD
10, 15455–15517, 2013

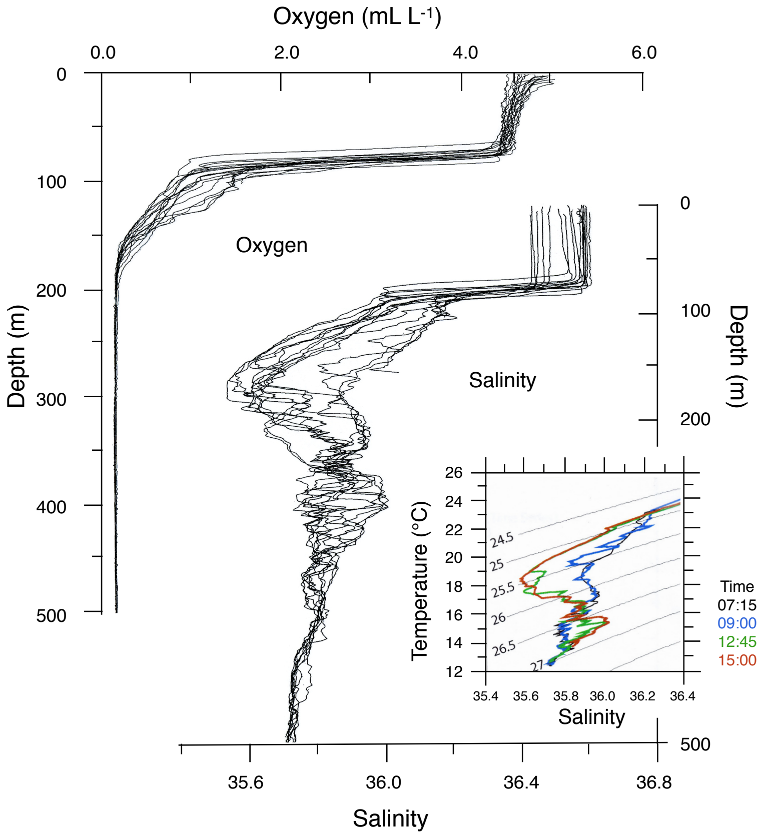

Fig. 2. Sta. 4010 of R/V *Sagar Sampada* near 19° N, 67° E (circle in Fig. 1) in January 1998. O_2 and salinity records from the CTD casts taken over 25 h, most of them hourly until 16:45. The ship drifted by about 41 km between the first and last casts. *T*-*S* diagram for four of the casts during the first 8 h (drift, about 13 km).

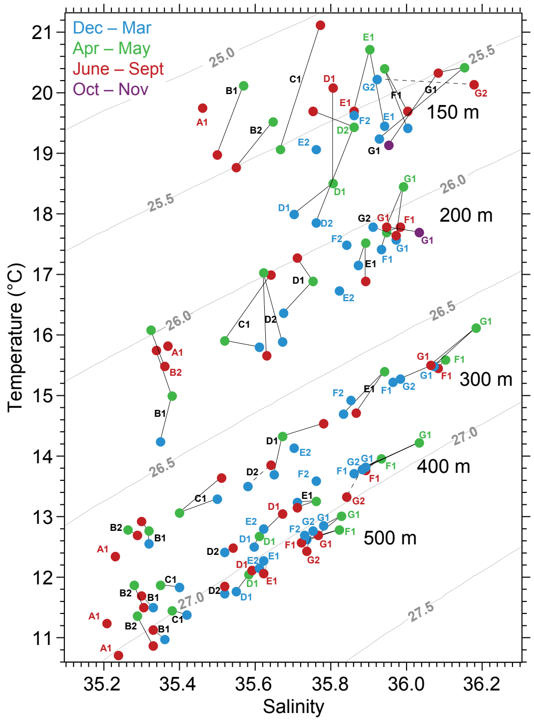

Fig. 3. *T*-*S* diagram for medians with ≥ 4 pairs per season of temperature and salinity in the boxes of our database (Table S.1.b). The seasons are defined as northeast monsoon, December–March (blue, NEM); spring intermonsoon, April–May (green, SI); southwest monsoon, June–September (red, SWM); and fall intermonsoon, October–November (purple, FI). Colored and black indices for single seasons and entire boxes, respectively. Adjoining seasons of each box connected by full lines, otherwise by broken lines. The slanted background lines are isopycnals (σ_t, kg m^{-3}).

BGD
10, 15455–15517, 2013

Oxygen minimum zone of the open Arabian Sea

K. Banse et al.

Title Page
Abstract | Introduction
Conclusions | References
Tables | Figures
◀◀ | ▶▶
◀ | ▶
Back | Close
Full Screen / Esc
Printer-friendly Version
Interactive Discussion

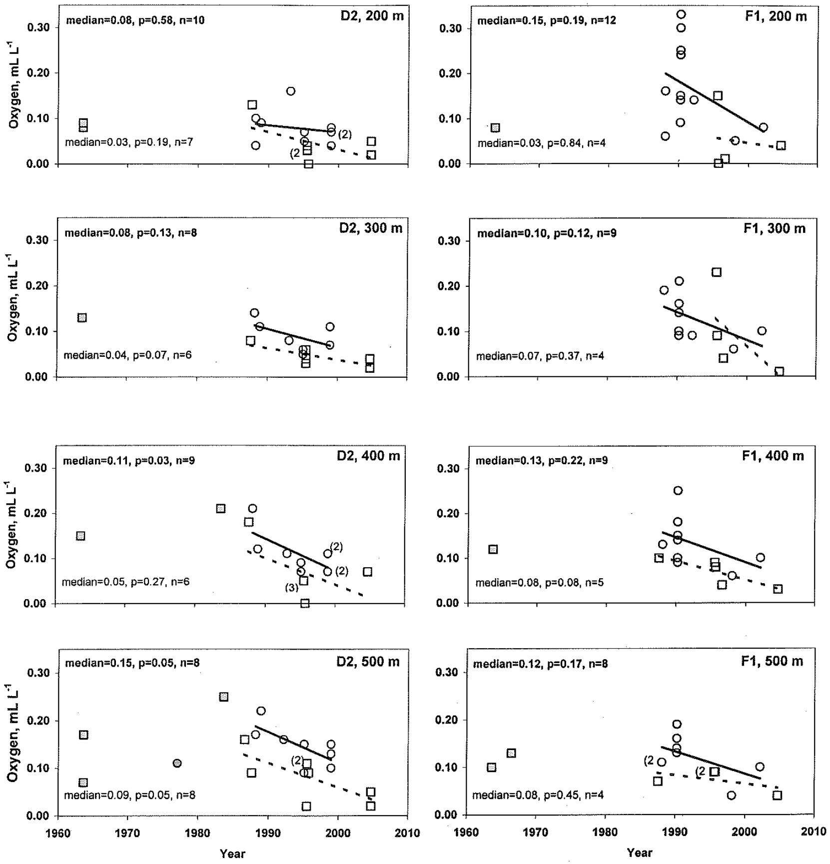

Fig. 4. Examples of regressions of oxygen observations on years for similar years with data for the NEM (circles, bold line, and text in upper part of panels) and SWM (squares, dashed line, and text in lower part of panels) for Boxes D2 and F1, chosen because two seasons were available for all depths, with medians, *p* for slopes, and number of values (*n*).

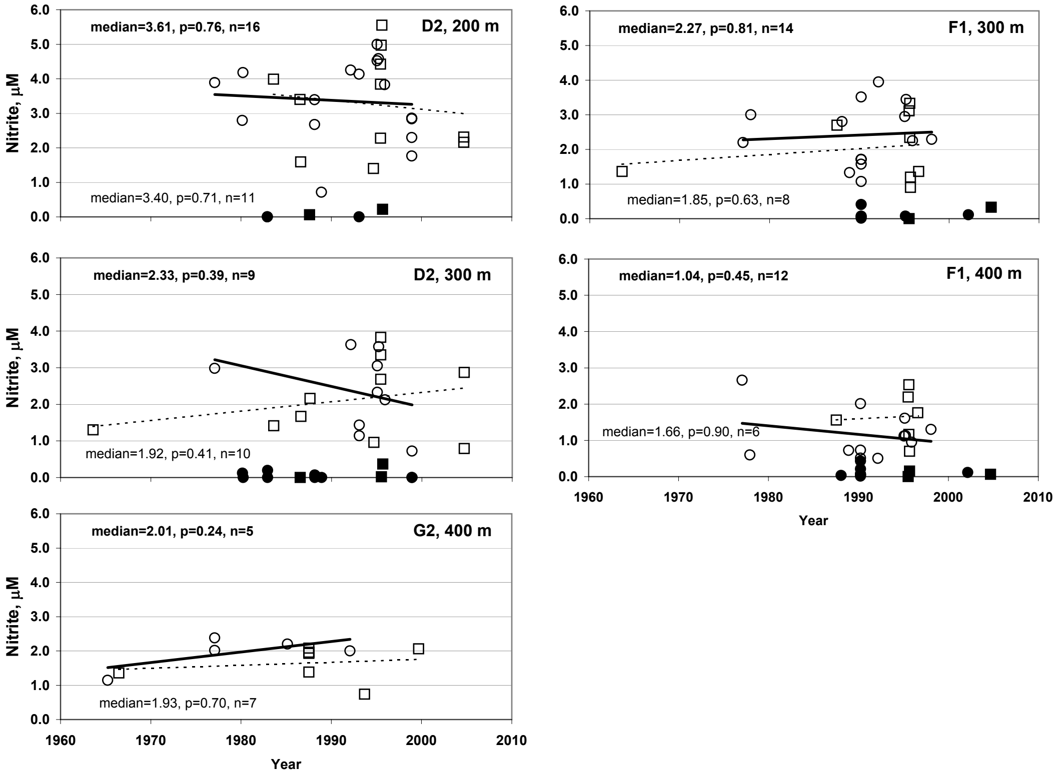

Fig. 5. Examples of regressions of ≥ 0.5 µM nitrite on years with data for the NEM (open circles, bold line, and text in upper part of panels) and SWM (open squares, dashed line, and text in lower part of panels) for Boxes D2 (two depths), F1 (two depths), and G2 (one depth), with medians, *p* for slopes, and number of values (all in Supplement, Table S.8, except for D2, 200 m, NEM). The < 0.5 µM values (filled symbols) are not part of the regressions (for text in panels see Fig. 4).

BGD
10, 15455–15517, 2013

Title Page
Abstract Introduction
Conclusions References
Tables Figures
◂◂ ▸▸
◂ ▸
Back Close
Full Screen / Esc
Printer-friendly Version
Interactive Discussion

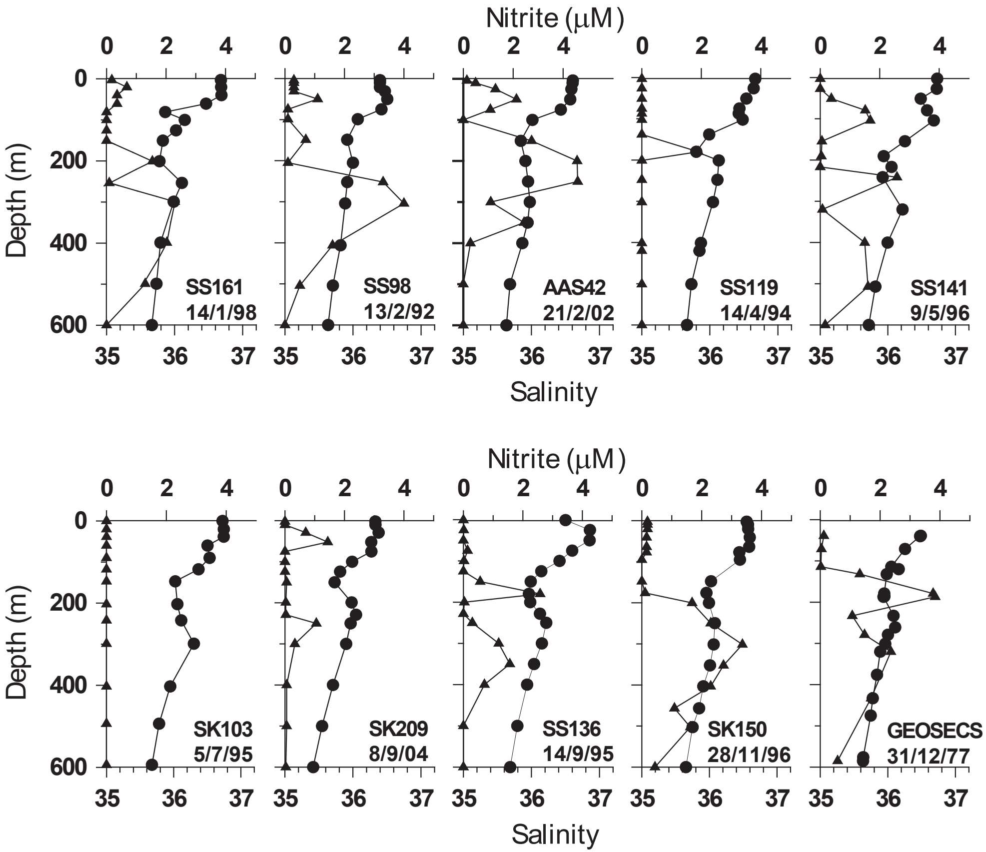

Fig. 6. Nitrite (triangles) and salinity (circles) to 600 m depth at the site of GEOSECS sta. 416 of 1977, revisited between 1992 and 2004 (panels arranged by month of visit; diamond in Fig. 1 marks the location).

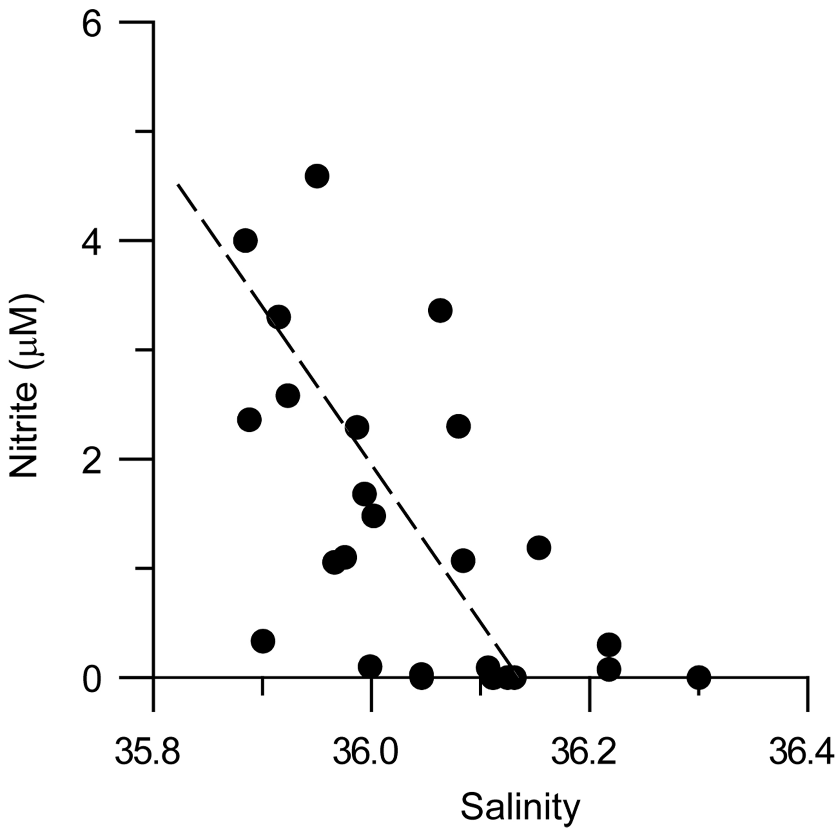

Fig. 7. Nitrite on salinity within and in the vicinity of the Persian Gulf salinity maximum (σ_t range, 26.18–26.74 kg m^{-3}) during the visits to the GEOSECS site shown in Fig. 6. The equation for the regression line is $NO_2^- = -14.566 \times \text{salinity} + 526.30$, $n = 26$.

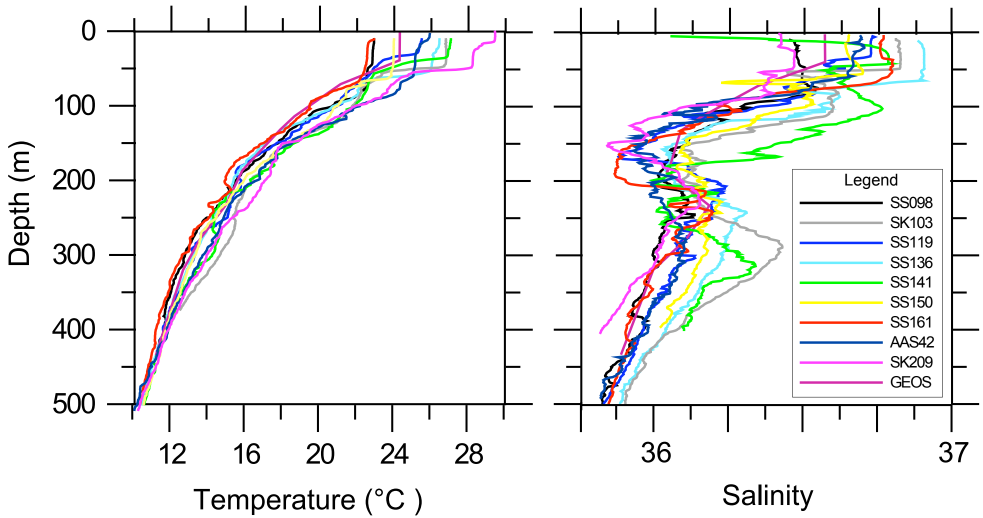

Fig. 8. Temperature and salinity records to 500 m depth during the visits to the GEOSECS site (for dates, see Fig. 6).

BGD
10, 15455–15517, 2013